


Cite this: *RSC Adv.*, 2023, 13, 30202

Design, synthesis and biological evaluation of tetrahydroquinoxaline sulfonamide derivatives as colchicine binding site inhibitors†

Haiyang Dong,^{‡a} Lu Lu,^{‡a} Xueting Song,^a Youkang Li,^a Jinguang Zhou,^b Yungen Xu,^c Yahong Zhang,^a Jianguo Qi,^a Tingting Liang^{✉a} and Jianhong Wang^{*a}

Colchicine binding site inhibitors (CBSIs) are potential microtubule targeting agents (MTAs), which can overcome multidrug resistance, improve aqueous solubility and reduce toxicity faced by most MTAs. Novel tetrahydroquinoxaline sulfonamide derivatives were designed, synthesized and evaluated for their antiproliferative activities. The MTT assay results demonstrated that some derivatives exhibited moderate to strong inhibitory activities against HT-29 cell line. Among them, compound I-7 was the most active compound. Moreover, I-7 inhibited tubulin polymerization, disturbed microtubule network, disrupted the formation of mitotic spindle and arrested cell cycle at G2/M phase. However, I-7 didn't induce cell apoptosis. Furthermore, the prediction of ADME demonstrated that I-7 showed favorable physiochemical and pharmacokinetic properties. And the detailed molecular docking confirmed I-7 targeted the site of colchicine through hydrogen and hydrophobic interactions.

Received 22nd August 2023

Accepted 9th October 2023

DOI: 10.1039/d3ra05720h

rsc.li/rsc-advances

1. Introduction

Cancer is a multifactorial disease and one of the two leading causes of death, and the incidence and mortality are rapidly growing worldwide. Based on the latest Global Cancer Statistics, there are an estimated 1.96 million new cases and nearly 0.61 million deaths in United States in 2023.¹ Therefore, it is imperative to develop new anticancer drugs, and chemotherapy, especially microtubule targeting agents (MTAs), have been successfully used for cancer treatment.² Microtubules are dynamic polymers composed of α and β heterodimer, and play important roles in many cellular functions such as maintaining cell shape, mitosis, cell movement and intracellular transport. MTAs promote or inhibit tubulin polymerization to interfere with tubulin dynamic and play anticancer efficacy.³ Up till now, some MTAs (*e.g.*, paclitaxel and vinorelbine) have been approved for treating various malignant tumors such as breast cancer and non-small cell lung cells.^{4,5} However, their clinical applications are hampered by multidrug resistance, toxicities and low bioavailability.^{6,7}

Colchicine binding site is located primarily within β tubulin and at the interface of α and β tubulin, which is shaped by strands S7, S8, S9 and S10, loop T7, helices H7 and H8 of β tubulin and loop T5 of α tubulin.^{8,9} The compounds which bind to the colchicine binding site inhibit the structural transition of curved-to-straight to prevent the microtubule formation.¹⁰ Recently, colchicine binding site inhibitors (CBSIs) have attracted more and more attentions in medicinal chemistry, due to the potential ability to circumvent the multidrug resistance associated with other MTAs such as taxane and vinca alkaloid binding site inhibitors.^{11–13} In addition to inducing G2/M phase arrest, CBSIs exhibit potent vascular disrupting effects.^{14–16} Over the past few years, many CBSIs have been reported, moreover, some of them have entered into clinical trials (Fig. 1).^{17–22} Nevertheless, no CBSIs have been approved for clinical applications because of systemic toxicities, inadequate efficacies or poor pharmacokinetic properties. Therefore, it is urgent to develop novel colchicine binding site inhibitors to conquer these limitations.

Sulfonamide derivatives are significant potential compounds with diverse biological activities, such as antibacterial, antiviral, antidepressant and anticancer.^{23–25} Initially, sulfonamides were developed as synthetic antibacterial agents to inhibit bacterial growth, for example sulfadimethoxine and sulfamethoxazole.²⁶ Subsequently, sulfonamide derivatives were found to act as diuretics, such as carbonic anhydrase inhibitors (acetazolamide), Na^+/Cl^- cotransport inhibitors (hydrochlorothiazide), $\text{Na}^+/\text{K}^+/\text{2Cl}^-$ cotransport inhibitors (furosemide).^{27,28} Moreover, sulfonamide derivatives also act as hypoglycemic drugs to promote

^aKey Laboratory of Natural Medicine and Immune-Engineering of Henan Province, Henan University Jinming Campus, Kaifeng 475004, Henan, China. E-mail: liangting910710@126.com

^bHuaihe Hospital of Henan University, Kaifeng 475004, Henan, China

^cDepartment of Medicinal Chemistry, Jiangsu Key Laboratory of Drug Design and Optimization, China Pharmaceutical University, Nanjing, 211198, China

† Electronic supplementary information (ESI) available. See DOI: <https://doi.org/10.1039/d3ra05720h>

‡ These authors contributed equally to this work.



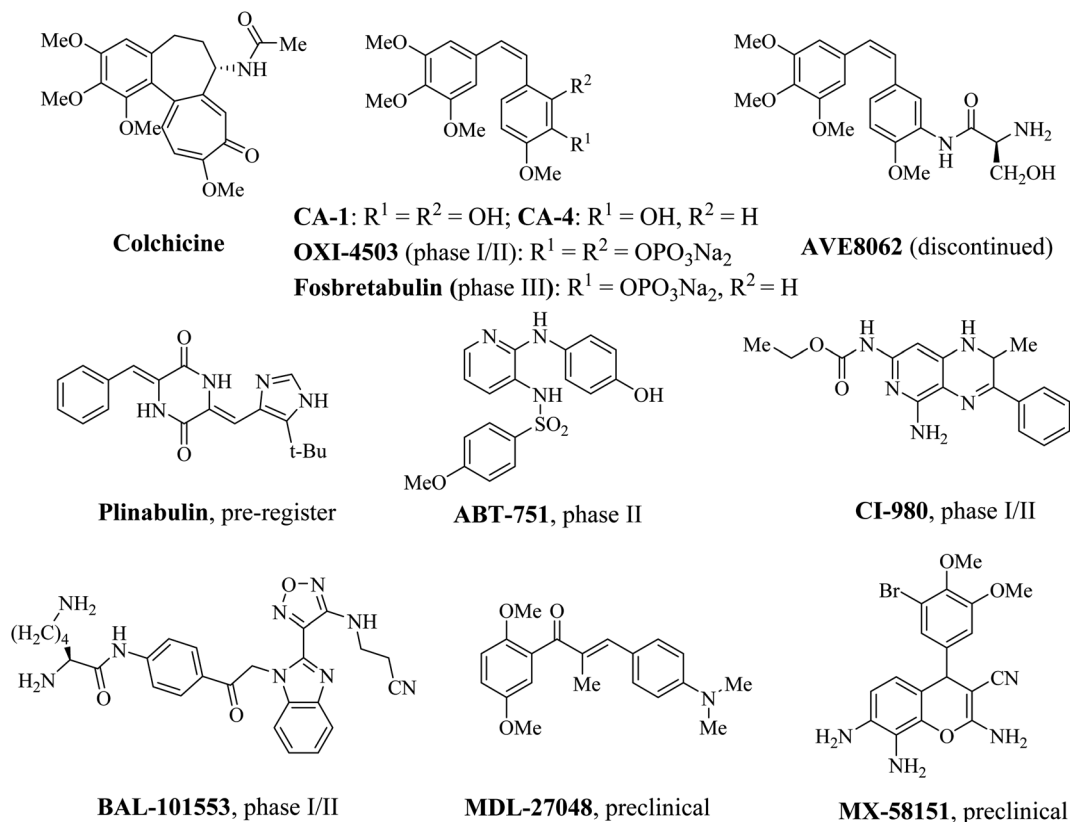


Fig. 1 Some representative colchicine binding site inhibitors (CBSIs).

insulin secretion (glimepiride).²⁹ In recent decades, some sulfonamides have been developed as anticancer agents, such as topoisomerase II poison amsacrine, HDAC inhibitor belinostat and JAK2/FLT3 dual inhibitor fedratinib (Fig. 2).^{30–32} As stated above, sulfonamide derivatives play significant roles in medicinal chemistry.

Our group have reported quinoxaline-2,3(1*H*,4*H*)-dione, 3,4-dihydroquinoxalin-2(1*H*)-one and 1,2,3,4-tetrahydroquinoxaline derivatives as colchicine binding site inhibitors (Fig. 3).^{33–35} In medicinal chemistry, bioisosterism is used as a common strategy for drug design, and sulfonamide moiety is an effective bioisostere for amide group. Therefore, based on our previous

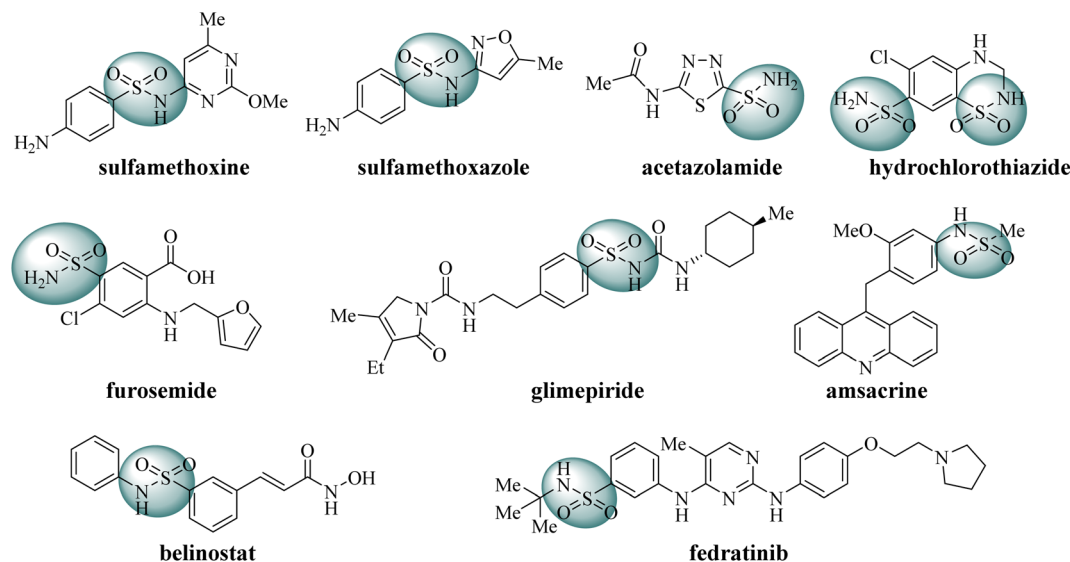


Fig. 2 Some representative FDA-approved drugs containing sulfonamide moiety.

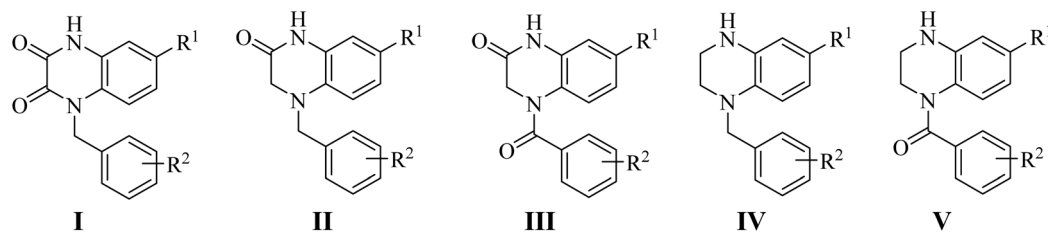


Fig. 3 Structures of CBSIs discovered by our group.

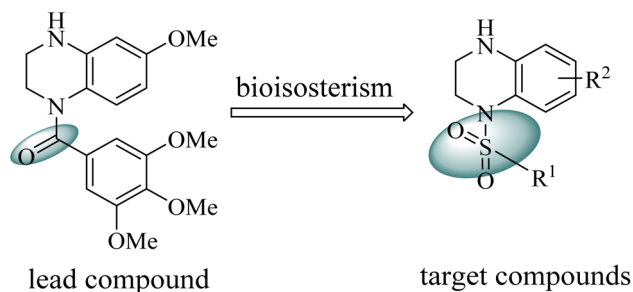
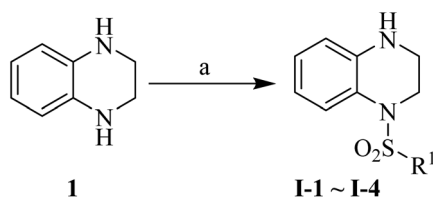


Fig. 4 Design of the target compounds.



Scheme 1 Reagents and conditions: (a) corresponding sulfonyl chloride, DMAP (cat.), TEA, anhydrous DCM, rt, 2 h.

work, we replaced the amide with the sulfonamide to design novel colchicine binding site inhibitors and complement the structure–activity relationships (Fig. 4). Herein, in this report, we described the design, synthesis and biological evaluations of tetrahydroquinoxaline sulfonamide derivatives. And the most

active compound was evaluated for the effects on tubulin polymerization, cell cycle and cell apoptosis. Moreover, the physicochemical and pharmacokinetic properties and the binding mode were predicted *in silico* studies.

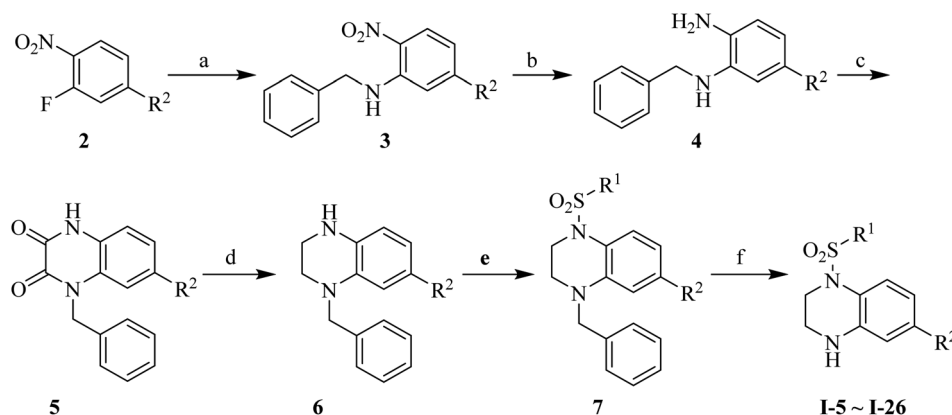
2. Results and discussion

2.1. Chemistry

Synthesis of the target compounds were presented in Schemes 1 and 2. Commercially available material 1,2,3,4-tetrahydroquinoxaline **1** was reacted with corresponding sulfonyl chloride in the presence of TEA and DMAP in anhydrous DCM to yield the target compounds **I-1–I-4** (Table 1). Raw materials **2** and benzylamine were reacted to synthesize intermediates **3**, which were reduced with hydrogen and Pd/C to produce diamines **4**. Diamines **4** were cyclized with diethyl oxalate to give intermediates **5**, followed by reduction to obtain intermediates **6**, which were reacted with corresponding sulfonyl chloride and subsequently deprotected with Raney Ni to furnish the target compounds **I-5–I-26** (Table 1).

2.2. Biological evaluations

2.2.1. *In vitro* cell growth inhibitory activities. The inhibitory activities of all compounds were evaluated towards human colon cancer cells HT-29 by MTT assay. The cell growth inhibitory ratio of HT-29 was assessed at the concentration of 1, 5 and 10 μ M after incubating for 48 h. As shown in Fig. 5, compounds



Scheme 2 Reagents and conditions: (a) benzylamine, K_2CO_3 , MeCN, reflux, 1.5 h; (b) 10% Pd/C, H_2 , MeOH, rt, 2 h; (c) diethyl oxalate, 140 $^\circ$ C, 4 h; (d) BH_3 –THF, anhydrous THF, 0 $^\circ$ C, 30 min then rt, 12 h; (e) corresponding sulfonyl chloride, DMAP (cat.), TEA, anhydrous DCM, rt, 2 h; (f) Raney Ni, H_2 , MeOH, 60 $^\circ$ C, 4 h.



Table 1 Structures of synthesized target compounds

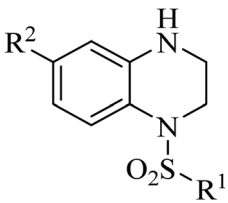
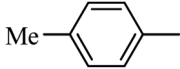
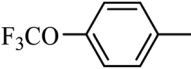
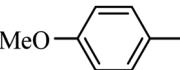
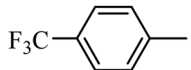
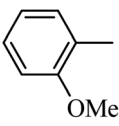
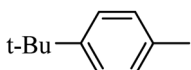
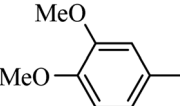
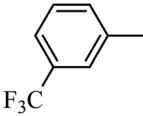
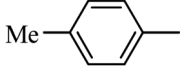
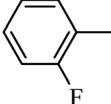
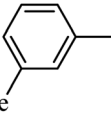
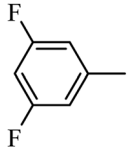
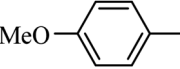
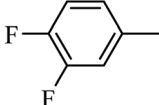
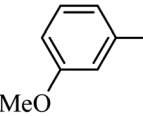
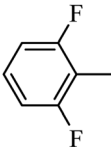
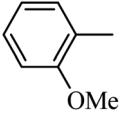
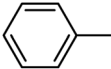
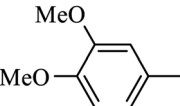
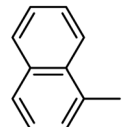
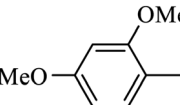
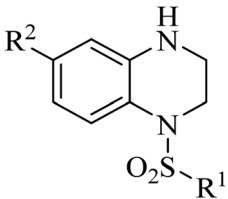
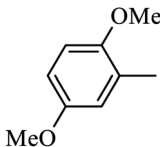
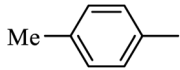
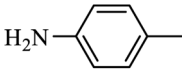
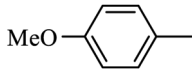
					
Compd	R ¹	R ²	Compd	R ¹	R ²
I-1		H	I-14		-OMe
I-2		H	I-15		-OMe
I-3		H	I-16		-OMe
I-4		H	I-17		-OMe
I-5		-OMe	I-18		-OMe
I-6		-OMe	I-19		-OMe
I-7		-OMe	I-20		-OMe
I-8		-OMe	I-21		-OMe
I-9		-OMe	I-22		-OMe
I-10		-OMe	I-23		-OMe
I-11		-OMe	I-24	Et	-OMe



Table 1 (Contd.)

					
Compd	R ¹	R ²	Compd	R ¹	R ²
I-12		-OMe	I-25		-COOMe
I-13		-OMe	I-26		-COOMe

I-6, I-7, I-17, I-19, I-21, I-23 and I-26 resulted in the more than 30% inhibition at the concentration of 10 μ M.

Preliminary structure–activity relationships were discussed as below. Compounds with methoxy group (R²) on the tetrahydroquinoxaline ring (I-5–I-24) exhibited better inhibitory activities than unsubstituted compounds (I-1–I-4) and compounds with methoxycarbonyl (I-25, I-26). When R² was methoxy group, R¹ was substituted phenyl group, the investigation focused on the property, position and number of substituents. Compounds with electron-donating groups (OMe, NH₂) or electron-withdrawing group (CF₃) at C4 position were more active than compound with larger group (*t*-Bu). Meanwhile, the number of substituents on the phenyl group have an important effect on the inhibitory activity. Disubstituted compounds (I-10, I-11) showed decreased activities compared with monosubstituted compound (I-7). However, difluorinated compounds (I-21) exhibited improved activities compared with monofluorinated

compound (I-18). Replacing the substituted phenyl group with naphthyl group produced compound I-23, which showed moderate antiproliferative activity. However, when the phenyl

Table 2 *In vitro* antiproliferative activities of I-7 and I-26

Compd	IC ₅₀ \pm SD ^a (μ M)			
	HT-29	HepG2	Hela	MCF-7
I-7	2.20 \pm 0.07	4.64 \pm 0.57	2.84 \pm 0.15	7.52 \pm 1.86
I-26	17.52 \pm 4.04	11.51 \pm 4.42	10.90 \pm 1.83	12.85 \pm 3.42
ABT-751	1.56 \pm 0.01	2.16 \pm 0.34	1.65 \pm 0.06	1.73 \pm 0.08

^a IC₅₀ values are indicated as the concentration that causes 50% inhibition of cell growth and are expressed as the means of at least three independent experiments.

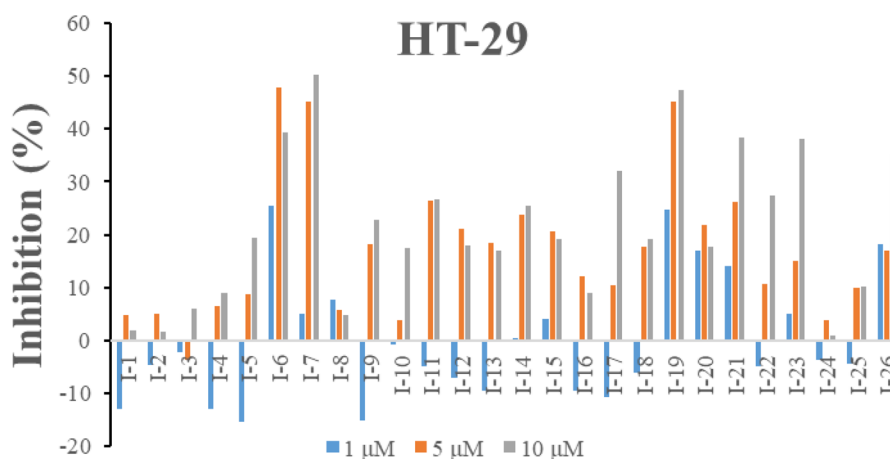


Fig. 5 Inhibition of all target compounds against HT-29 cells at the concentration of 1, 5 and 10 μ M after 48 h incubation.



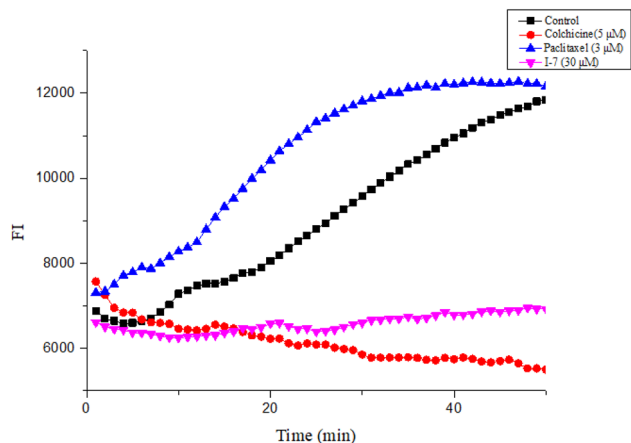


Fig. 6 Effect of compound I-7 on microtubule polymerization *in vitro*. Colchicine and paclitaxel were used as controls. The fluorescence was monitored at 37 °C after treated with these tested compounds.

group was replaced with ethyl group, compound I-24 totally lost the inhibitory activity.

On the basis of these analysis, compounds I-7 and I-26 were chosen to evaluate their antiproliferative activities against other

cancer cells, and ABT-751 was selected as the positive control. As described in Table 2, both compounds displayed the inhibitory activities against these four cancer cells, and I-7 showed stronger activity than I-26.

2.2.2. Compound I-7 inhibited tubulin polymerization.

Next, the tubulin polymerization assay was performed to evaluate the effect of I-7 on tubulin polymerization, while colchicine and paclitaxel were used as controls. As shown in Fig. 6, I-7 inhibited tubulin polymerization, which was similar with the microtubule depolymerization agent colchicine, while the microtubule polymerization agent paclitaxel promoted tubulin polymerization under the same condition, demonstrating that I-7 was able to inhibit tubulin polymerization *in vitro*.

Due to inhibition of tubulin polymerization would disturb the formation of microtubule network and destruct the cytoskeleton, immunofluorescence staining assay was subsequently performed to evaluate the effect of compounds on morphological characteristics of the microtubule in HT-29 cells. The cells were treated with compounds I-7 and I-26, taxol and CA-4 were used as controls. As shown in Fig. 7, both compounds could inhibit tubulin polymerization and disrupt microtubule morphology in HT-29 cells, which were similar to CA-4. In contrast, taxol played an opposite effect of promoting tubulin

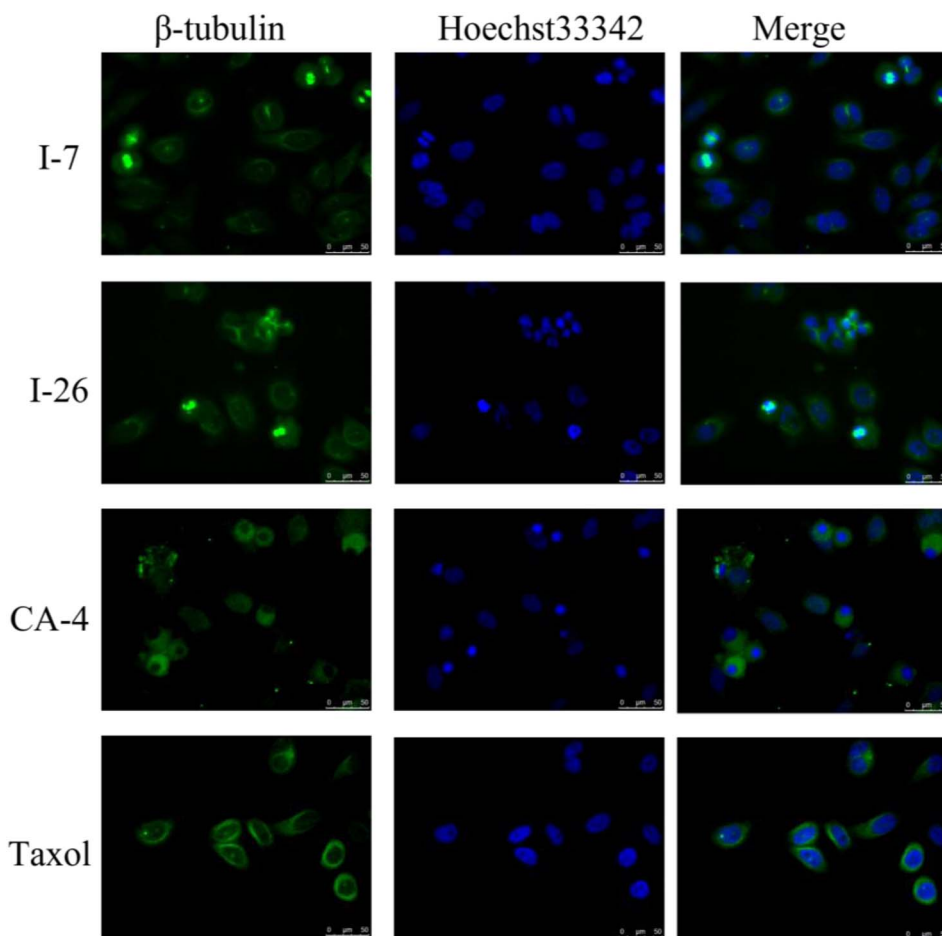


Fig. 7 Effects of compounds I-7 and I-26 on the cellular microtubule network and microtubule reassemble by immunofluorescence. CA-4 and taxol were used as controls. Cells were stained with Hoechst 33342 and anti- β -tubulin-Cy3 antibody.



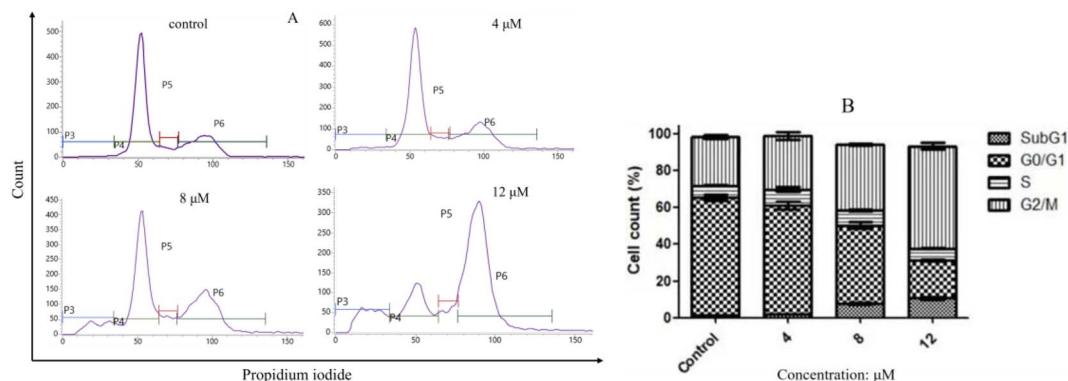


Fig. 8 Compound I-7 arrested cell cycle at G2/M phase in a concentration-dependent manner in HeLa cells. (A) HeLa cells were treated with I-7 at 4, 8 and 12 μM for 24 h, and the cell cycle was analyzed by flow cytometer with PI staining. (B) Cell cycle distribution.

polymerization and increasing microtubule bundles. In summary, it turned out that compounds **I-7** and **I-26** were microtubule depolymerization agents.

2.2.3. Compound I-7 arrested cell cycle at G2/M phase.

Flow cytometry analysis was used to investigate the effect of compound **I-7** on cell cycle progression with propidium iodide (PI) staining. As indicated in Fig. 8, compound **I-7** increased the proportion of cells in G2/M phase and reduced the proportion of cells in G0/G1 phase, implying **I-7** arrested cell cycle at G2/M phase in a concentration-dependent manner.

Table 3 Predicted ADME profile of compound I-7

Comp.	MW ^a	log P ^b	log Sw ^c	tPSA ^d	GI ^e	P-gp ^f	Lipinski ^g	Veber ^h
I-7	334.39	2.33	−3.5	76.25	High	No	0	0

^a Molecular weight. ^b log P was computed by the XLOGP3 method. ^c log Sw is water solubility calculated by the ESOL method. ^d Molecular polar surface area. ^e GI means gastrointestinal absorption. ^f P-gp means P-glycoprotein substrate. ^g Violation of the rule of five. ^h Veber's rule.

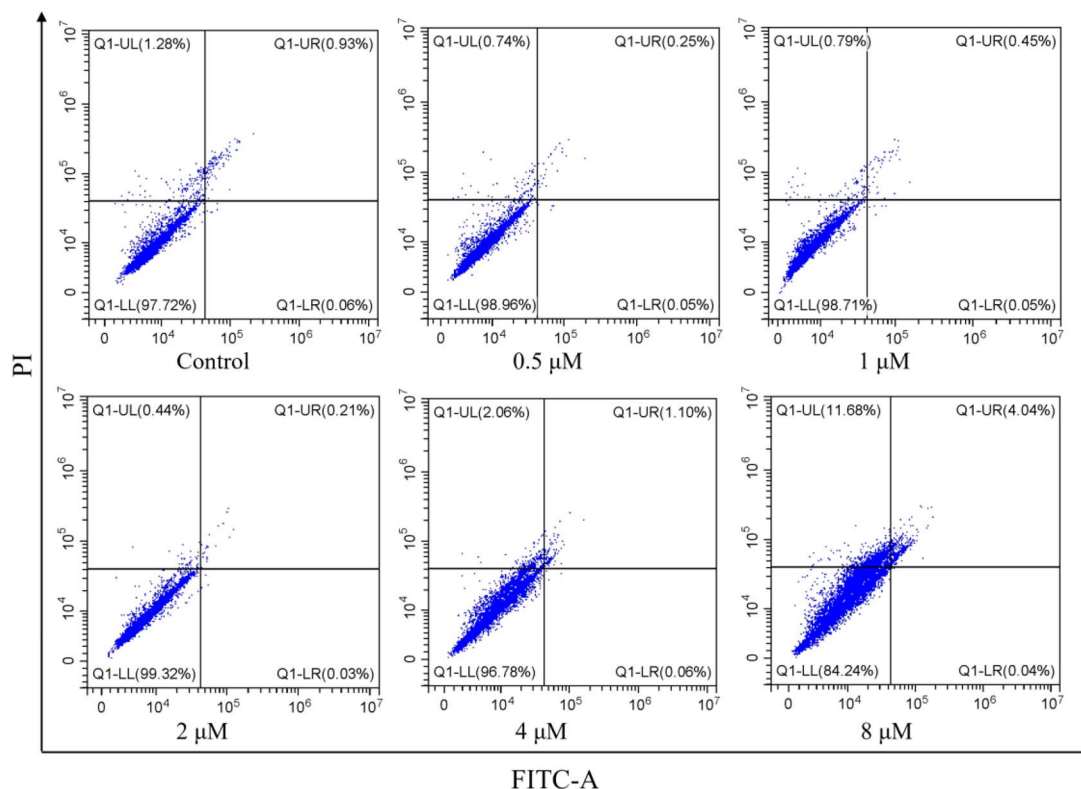


Fig. 9 Effect of apoptosis in HeLa cells induced by I-7. HeLa cells were treated with I-7 at 0.5, 1, 2, 4 and 8 μM for 48 h. The cells were harvested, stained with annexin-V FITC and PI, and analyzed by flow cytometry.



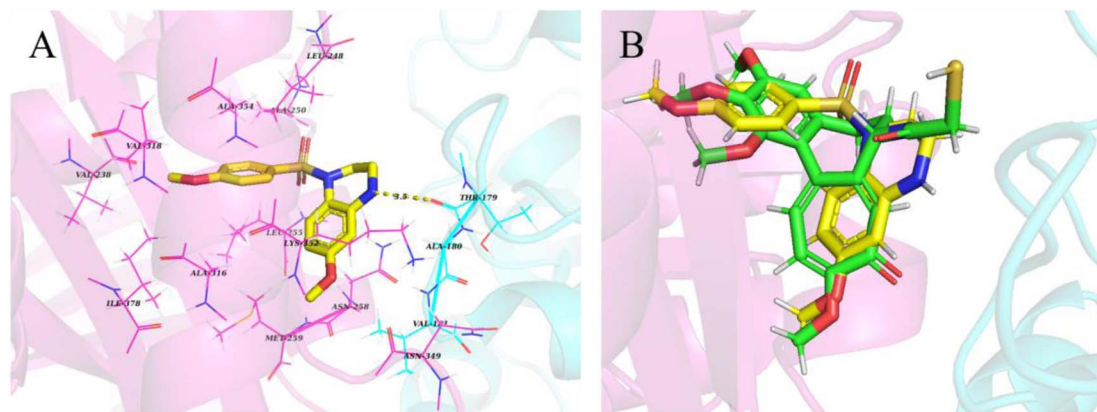


Fig. 10 (A) Proposed binding mode of the most active compound I-7 in the binding site of tubulin (PDB: 1SA0). (B) Overlap of compound I-7 (yellow) and DAMA-colchicine (green).

2.2.4. Effect of apoptosis induced by I-7. Cell apoptosis is the main form of cell death after the cells were treated with microtubule depolymerization agents to arrest cell cycle at G2/M phase. Therefore, to evaluate whether I-7 could trigger cell apoptosis, flow cytometric assay was used for I-7 on HeLa cells. As shown in Fig. 9, the population of apoptotic cells was relatively small even though the concentration of I-7 was up to 8 μM , suggesting that I-7 didn't trigger cell apoptosis, instead of other cell death such as ferroptosis and necrosis, which was different with our previous reported compounds.

2.2.5. Prediction of druglike properties of I-7. The ADME profile of the most potent compound I-7 was predicted using the web tool SwissADME.³⁶ As demonstrated in Table 3, I-7 was predicted to exhibit promising physicochemical and pharmacokinetic properties as it did not violate the Lipinski and Veber rules, and showed moderate water solubility and high intestinal absorbance (log *P* value measured by the shake-flask method is 1.15). Meanwhile, based on the predicted results, I-7 was not the substrate of P-gp, a transmembrane efflux transporter, implying I-7 may overcome drug resistance caused by the multidrug resistance (MDR) efflux pump.

2.2.6. Binding mode of compound I-7 with tubulin. To investigate the binding mode of tetrahydroquinoxaline sulfonamide derivatives with tubulin, molecular docking study was carried out using Maestro 11.5. The cocrystal structure of tubulin with DAMA-colchicine (PDB: 1SA0) was obtained from RCSB protein bank. As demonstrated in Fig. 10, tetrahydroquinoxaline group was located at the interface of α and β tubulin, and formed hydrophobic interaction with βAsn258 , βMet259 and βLys352 . Besides these, one hydrogen bond was formed between NH and αThr179 . Meanwhile, 4-methoxy phenyl was occupied in a deeply hydrophobic pocket in β tubulin.

3. Conclusions

In the present study, we disclosed the design, synthesis and biological evaluation of tetrahydroquinoxaline sulfonamide derivatives based on our previous work. Antiproliferative assays suggested that some of these synthesized compounds displayed

moderate to strong inhibitory activities and structure–activity relationships were summarized. Among all these target compounds, compound I-7 exhibited excellent antiproliferative activities against all tested cancer cells. Further biological analyses demonstrated that compound I-7 inhibited tubulin polymerization and arrested cell cycle at G2/M phase. However, compound I-7 didn't induce cell apoptosis after mitotic arrest, instead of other cell death. Besides these, physicochemical and pharmacokinetic properties were predicted by SwissADME, and the predicted results demonstrated that I-7 had satisfactory drug-like criteria and deserved further modification. In addition, molecular docking study predicted the binding mode of compound I-7 with the colchicine binding site. Taken together, compound I-7 was a potent colchicine binding site inhibitor.

4. Materials and methods

4.1. Chemistry

4.1.1. General information. Unless otherwise specified, all solvents and reagents were commercially obtained and used without further purification. Thin layer chromatography was used to monitor the reactions. And the reactions were purified by flash column chromatography. All synthesized compounds were verified by NMR and HRMS. ^1H NMR (300 MHz) and ^{13}C NMR (75 MHz) spectra were recorded with Bruker ADVANCE 300 and referenced to deuterium chloroform (CDCl_3) or deuterium dimethyl sulfoxide ($\text{DMSO}-d_6$). The coupling constants *J* were reported in Hertz (Hz), and the splitting abbreviations used were as follows: singlet (s), doublet (d), triplet (t), multiplet (m), broad resonances (br). High-resolution mass spectra (HRMS) were tested on Thermo Q Exactive Focus mass spectrometer. Purity of the target compounds were detected by HPLC system, the detailed method is as follow: Instrument: SHIMADZU Labsolutions instrument with an BDS Hypersil C18 column (4.6 mm \times 250 mm, 5 μm); wave length: 254 nm; temperature: 30 $^\circ\text{C}$; flow rate: 1.0 mL min^{-1} ; injection: 20 μL ; mobile phase: A phase: H_2O ; B phase: MeOH; isocratic elution: 95% MeOH + 5% H_2O .

4.1.2. Synthesis of *N*-benzyl-5-methoxy-2-nitroaniline (3-1). To a solution of benzylamine (2.07 g, 19.28 mmol) in MeCN (40

mL) was added 3-fluoro-4-nitroanisole (3.00 g, 17.50 mmol) and K_2CO_3 (4.84 g, 35.02 mmol), then the mixture was refluxed until the starting materials disappeared on TLC (PE : EtOAc = 5 : 1). Once the reaction was complete, the reaction mixture was cooled to room temperature, filtrated. The filtrate was washed with water (20 mL \times 3) and brine (20 mL \times 3), dried with Na_2SO_4 , filtered and evaporated to produce a crude product (3.92 g, 86.6%) as a yellow solid. Without further purification, the crude intermediate was used directly. 1H NMR (300 MHz, $DMSO-d_6$) δ 8.87 (t, J = 5.7 Hz, 1H), 8.06 (d, J = 9.7 Hz, 1H), 7.46–7.41 (m, 2H), 7.40–7.34 (m, 2H), 7.32–7.27 (m, 1H), 6.35–6.25 (m, 2H), 4.64 (d, J = 5.9 Hz, 2H), 3.74 (s, 3H).

4.1.3. Synthesis of methyl 3-(benzylamino)-4-nitrobenzoate (3-2). Orange solid (1.21 g, 84.2%). 1H NMR (300 MHz, $CDCl_3$) δ 8.34 (t, J = 5.6 Hz, 1H), 8.24 (d, J = 8.9 Hz, 1H), 7.59 (d, J = 1.5 Hz, 1H), 7.41–7.30 (m, 5H), 7.26 (dd, J = 8.9, 1.7 Hz, 1H), 4.59 (d, J = 5.5 Hz, 2H), 3.91 (s, 3H).

Synthesis of intermediates **4-1**, **4-2**, **5-1**, **5-2**, **6-1** and **6-2** were similar with the methods reported by our previous published literature.³⁵

4.1.4. Synthesis of N^1 -benzyl-5-methoxybenzene-1,2-diamine (4-1). Gray oil (679 mg, 93.9%). 1H NMR (300 MHz, $CDCl_3$) δ 7.50–7.35 (m, 5H), 6.73 (d, J = 8.3 Hz, 1H), 6.36 (d, J = 2.7 Hz, 1H), 6.28 (dd, J = 8.3, 2.7 Hz, 1H), 4.37 (s, 2H), 3.79 (s, 3H), 3.16 (br, 3H).

4.1.5. Synthesis of methyl 4-amino-3-(benzylamino)benzoate (4-2). Orange oil (0.75 g, 70.1%). 1H NMR (300 MHz, $CDCl_3$) δ 7.48 (dd, J = 8.0, 1.8 Hz, 1H), 7.45–7.27 (m, 6H), 6.71 (d, J = 8.0 Hz, 1H), 4.33 (s, 2H), 3.85 (s, 3H), 3.78 (br, 2H), 3.41 (s, 1H).

4.1.6. Synthesis of 1-benzyl-7-methoxy-1,4-dihydroquinoxaline-2,3-dione (5-1). Brown solid (95 mg, 76.9%). Without further purification, the crude intermediate was used directly.

4.1.7. Synthesis of methyl 4-benzyl-2,3-dioxo-1,2,3,4-tetrahydroquinoxaline-6-carboxylate (5-2). Offwhite solid (857 mg, 70.8%).

4.1.8. Synthesis of 1-benzyl-7-methoxy-1,2,3,4-tetrahydroquinoxaline (6-1). White solid (0.35 g, 38.8%). 1H NMR (300 MHz, $CDCl_3$) δ 7.28–7.14 (m, 6H), 6.39 (d, J = 8.3 Hz, 1H), 6.14–6.00 (m, 2H), 4.36 (s, 2H), 3.57 (s, 3H), 3.33 (s, 4H).

4.1.9. Synthesis of methyl 4-benzyl-1,2,3,4-tetrahydroquinoxaline-6-carboxylate (6-2). Yellow oil (490 mg, 67.3%). 1H NMR (300 MHz, $CDCl_3$) δ 7.36–7.21 (m, 7H), 6.42 (d, J = 8.0 Hz, 1H), 4.42 (s, 2H), 4.28 (s, 1H), 3.77 (s, 3H), 3.40 (t, J = 5.1 Hz, 2H), 3.22 (t, J = 5.1 Hz, 2H).

4.1.10. Synthesis of 4-benzyl-6-methoxy-1,2,3,4-tetrahydroquinoxaline (7-1). To the solution of **6-1** (300 mg, 1.18 mmol) in DCM (40 mL) was added DMAP (43 mg, 0.35 mmol), TEA (239 mg, 2.36 mmol), the reaction mixture was cooled to 0 °C, then tosyl chloride (248 mg, 1.30 mmol) in DCM was added to the reaction mixture. The mixture was stirred at room temperature for 2 h and monitored by TLC. Then the mixture was concentrated and re-dissolved with EtOAc (20 mL), washed with 0.1 mol L^{-1} HCl (20 mL \times 3), water (20 mL \times 3) and brine (20 mL \times 3), dried over Na_2SO_4 , filtered and evaporated to obtain **7-1** (406 mg, 81.8%) as a white solid. 1H NMR

(300 MHz, $CDCl_3$) δ 7.64 (d, J = 8.8 Hz, 1H), 7.48 (d, J = 8.3 Hz, 2H), 7.29–7.20 (m, 5H), 6.89–6.82 (m, 2H), 6.32 (dd, J = 8.9, 2.7 Hz, 1H), 6.10 (d, J = 2.7 Hz, 1H), 4.26 (s, 2H), 3.90 (t, J = 5.4 Hz, 2H), 3.73 (s, 3H), 2.98 (t, J = 5.4 Hz, 2H), 2.47 (s, 3H).

Intermediates **7-2**–**7-21** and the target compounds **I-1**–**I-4** were synthesized following a similar method of compound **7-1**.

4.1.11. Synthesis of 4-benzyl-6-methoxy-1-((*m*-tolylsulfonyl)-1,2,3,4-tetrahydroquinoxaline (7-2). White solid (407 mg, 83.3%). 1H NMR (300 MHz, $CDCl_3$) δ 7.64–7.55 (m, 1H), 7.42–7.28 (m, 4H), 7.24–7.16 (m, 3H), 6.85–6.74 (m, 2H), 6.33–6.25 (m, 1H), 6.09–6.03 (m, 1H), 4.20 (s, 2H), 3.86 (t, J = 5.6 Hz, 2H), 3.69 (s, 3H), 2.95 (t, J = 5.2 Hz, 2H), 2.32 (s, 3H).

4.1.12. Synthesis of 4-benzyl-6-methoxy-1-((4-methoxyphenyl)sulfonyl)-1,2,3,4-tetrahydroquinoxaline (7-3). White solid (393 mg, 78.4%). 1H NMR (300 MHz, $CDCl_3$) δ 7.59 (d, J = 8.8 Hz, 1H), 7.46 (d, J = 8.9 Hz, 2H), 7.23–7.14 (m, 3H), 6.87 (d, J = 8.9 Hz, 2H), 6.82–6.72 (m, 2H), 6.26 (dd, J = 8.8, 2.7 Hz, 1H), 6.04 (d, J = 2.6 Hz, 1H), 4.24 (s, 2H), 3.88–3.83 (m, 5H), 3.68 (s, 3H), 2.98 (t, J = 5.4 Hz, 2H).

4.1.13. Synthesis of 4-benzyl-6-methoxy-1-((3-methoxyphenyl)sulfonyl)-1,2,3,4-tetrahydroquinoxaline (7-4). White solid (417 mg, 77.2%). 1H NMR (300 MHz, $CDCl_3$) δ 7.62 (d, J = 8.8 Hz, 1H), 7.36–7.27 (m, 1H), 7.24–7.16 (m, 4H), 7.13–7.05 (m, 1H), 6.93–6.88 (m, 1H), 6.82–6.74 (m, 2H), 6.28 (dd, J = 8.8, 2.4 Hz, 1H), 6.05 (d, J = 2.3 Hz, 1H), 4.21 (s, 2H), 3.86 (t, J = 5.9 Hz, 2H), 3.67 (s, 3H), 3.60 (s, 3H), 2.94 (t, J = 5.3 Hz, 2H).

4.1.14. Synthesis of 4-benzyl-6-methoxy-1-((2-methoxyphenyl)sulfonyl)-1,2,3,4-tetrahydroquinoxaline (7-5). White solid (412 mg, 82.2%). 1H NMR (300 MHz, $CDCl_3$) δ 7.95 (dd, J = 7.8, 1.7 Hz, 1H), 7.58–7.48 (m, 1H), 7.36 (d, J = 8.8 Hz, 1H), 7.31–7.23 (m, 3H), 7.09–6.99 (m, 3H), 6.89 (d, J = 8.3 Hz, 1H), 6.22 (dd, J = 8.8, 2.7 Hz, 1H), 6.15 (d, J = 2.7 Hz, 1H), 4.37 (s, 2H), 3.85 (t, J = 5.2 Hz, 2H), 3.67 (s, 3H), 3.49 (s, 3H), 3.12 (t, J = 5.2 Hz, 2H).

4.1.15. Synthesis of 4-benzyl-1-((3,4-dimethoxyphenyl)sulfonyl)-6-methoxy-1,2,3,4-tetrahydroquinoxaline (7-6). White solid (424 mg, 56.9%). 1H NMR (300 MHz, $CDCl_3$) δ 7.68 (d, J = 8.8 Hz, 1H), 7.39–7.30 (m, 2H), 7.26–7.23 (m, 2H), 6.89 (d, J = 8.5 Hz, 1H), 6.82–6.76 (m, 3H), 6.32 (dd, J = 8.8, 2.7 Hz, 1H), 6.08 (d, J = 2.7 Hz, 1H), 4.28 (s, 2H), 3.97 (s, 3H), 3.90 (t, J = 5.4 Hz, 2H), 3.71 (s, 3H), 3.62 (s, 3H), 3.01 (t, J = 5.4 Hz, 2H).

4.1.16. Synthesis of 4-benzyl-1-((2,4-dimethoxyphenyl)sulfonyl)-6-methoxy-1,2,3,4-tetrahydroquinoxaline (7-7). White solid (444 mg, 72.8%). 1H NMR (300 MHz, $CDCl_3$) δ 7.81 (d, J = 8.7 Hz, 1H), 7.39 (d, J = 8.7 Hz, 1H), 7.31–7.15 (m, 3H), 7.02 (d, J = 6.9 Hz, 2H), 6.47 (dd, J = 8.8, 2.3 Hz, 1H), 6.36 (d, J = 2.3 Hz, 1H), 6.19 (dd, J = 8.8, 2.6 Hz, 1H), 6.13 (d, J = 2.7 Hz, 1H), 4.35 (s, 2H), 3.88–3.75 (m, 5H), 3.63 (s, 3H), 3.40 (s, 3H), 3.09 (t, J = 5.1 Hz, 2H).

4.1.17. Synthesis of 4-benzyl-1-((2,5-dimethoxyphenyl)sulfonyl)-6-methoxy-1,2,3,4-tetrahydroquinoxaline (7-8). White solid (450 mg, 84.4%). 1H NMR (300 MHz, $CDCl_3$) δ 7.38 (d, J = 3.2 Hz, 1H), 7.29 (d, J = 8.8 Hz, 1H), 7.20–7.14 (m, 3H), 7.02–6.94 (m, 3H), 6.76 (d, J = 9.0 Hz, 1H), 6.14 (dd, J = 8.8, 2.6 Hz, 1H), 6.07 (d, J = 2.6 Hz, 1H), 4.29 (s, 2H), 3.76 (t, J = 5.3 Hz, 2H), 3.68 (s, 3H), 3.58 (s, 3H), 3.38 (s, 3H), 3.06 (t, J = 5.2 Hz, 2H).



4.1.18. Synthesis of 4-benzyl-6-methoxy-1-((4-nitrophenyl)sulfonyl)-1,2,3,4-tetra-hydroquinoxaline (7-9). White solid (427 mg, 69.0%). ^1H NMR (300 MHz, CDCl_3) δ 8.19 (d, J = 8.8 Hz, 2H), 7.66 (d, J = 8.8 Hz, 2H), 7.59 (d, J = 8.8 Hz, 1H), 7.20–7.10 (m, 3H), 6.84–6.76 (m, 2H), 6.31 (dd, J = 8.9, 2.6 Hz, 1H), 6.17 (d, J = 2.6 Hz, 1H), 4.20 (s, 2H), 3.92 (t, J = 5.4 Hz, 2H), 3.73 (s, 3H), 2.94 (t, J = 5.5 Hz, 2H).

4.1.19. Synthesis of 4-benzyl-6-methoxy-1-((4-(trifluoromethoxy)phenyl)sulfonyl)-1,2,3,4-tetrahydroquinoxaline (7-10). White solid (385 mg, 68.3%). ^1H NMR (300 MHz, CDCl_3) δ 7.66–7.58 (m, 3H), 7.31–7.25 (m, 5H), 6.93–6.86 (m, 2H), 6.34 (dd, J = 8.9, 2.7 Hz, 1H), 6.13 (d, J = 2.7 Hz, 1H), 4.21 (s, 2H), 3.92 (t, J = 5.5 Hz, 2H), 3.75 (s, 3H), 2.99 (t, J = 5.5 Hz, 2H).

4.1.20. Synthesis of 4-benzyl-6-methoxy-1-((4-(trifluoromethyl)phenyl)sulfonyl)-1,2,3,4-tetrahydroquinoxaline (7-11). White solid (464 mg, 70.2%). ^1H NMR (300 MHz, CDCl_3) δ 7.73–7.63 (m, 4H), 7.59 (d, J = 8.9 Hz, 1H), 7.24–7.17 (m, 3H), 6.85–6.78 (m, 2H), 6.30 (dd, J = 8.9, 2.6 Hz, 1H), 6.09 (d, J = 2.6 Hz, 1H), 4.18 (s, 2H), 3.89 (t, J = 5.4 Hz, 2H), 3.70 (s, 3H), 2.94 (t, J = 5.5 Hz, 2H).

4.1.21. Synthesis of 4-benzyl-1-((4-*tert*-butyl)phenyl)sulfonyl)-6-methoxy-1,2,3,4-tetrahydroquinoxaline (7-12). White solid (442 mg, 76.4%). ^1H NMR (300 MHz, CDCl_3) δ 7.61 (d, J = 8.8 Hz, 1H), 7.55–7.46 (m, 4H), 7.29–7.23 (m, 3H), 7.00–6.94 (m, 2H), 6.33 (dd, J = 8.8, 2.7 Hz, 1H), 6.11 (d, J = 2.7 Hz, 1H), 4.16 (s, 2H), 3.88 (t, J = 5.4 Hz, 2H), 3.74 (s, 3H), 2.92 (t, J = 5.5 Hz, 2H), 1.37 (s, 9H).

4.1.22. Synthesis of 4-benzyl-6-methoxy-1-((3-(trifluoromethyl)phenyl)sulfonyl)-1,2,3,4-tetrahydroquinoxaline (7-13). White solid (449 mg, 71.4%). ^1H NMR (300 MHz, CDCl_3) δ 7.90 (d, J = 7.8 Hz, 1H), 7.81–7.59 (m, 2H), 7.59 (dd, J = 7.8, 1.4 Hz, 1H), 7.32–7.18 (m, 4H), 6.96 (dd, J = 7.2, 2.4 Hz, 2H), 6.20 (dd, J = 8.8, 2.6 Hz, 1H), 6.14 (d, J = 2.6 Hz, 1H), 4.33 (s, 2H), 3.91 (t, J = 5.3 Hz, 2H), 3.68 (s, 3H), 3.15 (t, J = 5.3 Hz, 2H).

4.1.23. Synthesis of 4-benzyl-1-((2-fluorophenyl)sulfonyl)-6-methoxy-1,2,3,4-tetrahydroquinoxaline (7-14). White solid (357 mg, 73.5%). ^1H NMR (300 MHz, CDCl_3) δ 7.82 (ddd, J = 7.9, 6.9, 1.8 Hz, 1H), 7.66–7.56 (m, 1H), 7.47 (d, J = 8.8 Hz, 1H), 7.33–7.24 (m, 4H), 7.22–7.14 (m, 1H), 6.99 (dd, J = 6.7, 2.8 Hz, 2H), 6.28 (dd, J = 8.8, 2.7 Hz, 1H), 6.18 (d, J = 2.7 Hz, 1H), 4.40 (s, 2H), 3.98 (t, J = 5.3 Hz, 2H), 3.71 (s, 3H), 3.25 (t, J = 5.4 Hz, 2H).

4.1.24. Synthesis of 4-benzyl-1-((3,5-difluorophenyl)sulfonyl)-6-methoxy-1,2,3,4-tetrahydroquinoxaline (7-15). White solid (421 mg, 75.9%). ^1H NMR (300 MHz, CDCl_3) δ 7.55 (d, J = 8.8 Hz, 1H), 7.29–7.18 (m, 3H), 7.13–7.02 (m, 2H), 6.97 (d, J = 2.3 Hz, 1H), 6.93–6.81 (m, 2H), 6.30 (dd, J = 8.9, 2.7 Hz, 1H), 6.14 (d, J = 2.7 Hz, 1H), 4.27 (s, 2H), 3.87 (t, J = 5.5 Hz, 2H), 3.71 (s, 3H), 2.99 (t, J = 5.5 Hz, 2H).

4.1.25. Synthesis of 4-benzyl-1-((3,4-difluorophenyl)sulfonyl)-6-methoxy-1,2,3,4-tetrahydroquinoxaline (7-16). White solid (424 mg, 78.6%). ^1H NMR (300 MHz, CDCl_3) δ 7.55 (d, J = 8.8 Hz, 1H), 7.39–7.31 (m, 1H), 7.30–7.20 (m, 4H), 7.17–7.10 (m, 1H), 6.88–6.80 (m, 2H), 6.28 (dd, J = 8.9, 2.6 Hz, 1H),

6.14 (d, J = 2.6 Hz, 1H), 4.25 (s, 2H), 3.87 (t, J = 5.4 Hz, 2H), 3.70 (s, 3H), 2.98 (t, J = 5.5 Hz, 2H).

4.1.26. Synthesis of 4-benzyl-1-((2,6-difluorophenyl)sulfonyl)-6-methoxy-1,2,3,4-tetrahydroquinoxaline (7-17). White solid (427 mg, 81.2%). ^1H NMR (300 MHz, CDCl_3) δ 7.54–7.38 (m, 2H), 7.27–7.17 (m, 3H), 7.02–6.89 (m, 4H), 6.22 (dd, J = 8.8, 2.7 Hz, 1H), 6.14 (d, J = 2.7 Hz, 1H), 4.36 (s, 2H), 3.97 (t, J = 5.0 Hz, 2H), 3.65 (s, 3H), 3.27 (t, J = 5.0 Hz, 2H).

4.1.27. Synthesis of 4-benzyl-6-methoxy-1-(phenylsulfonyl)-1,2,3,4-tetrahydroquinoxaline (7-18). White solid (395 mg, 84.5%). ^1H NMR (300 MHz, CDCl_3) δ 7.67–7.56 (m, 4H), 7.51–7.43 (m, 2H), 7.27–7.20 (m, 3H), 6.86–6.78 (m, 2H), 6.33 (dd, J = 8.9, 2.7 Hz, 1H), 6.09 (d, J = 2.7 Hz, 1H), 4.23 (s, 2H), 3.92 (t, J = 5.5 Hz, 2H), 3.73 (s, 3H), 2.97 (t, J = 5.5 Hz, 2H).

4.1.28. Synthesis of 4-benzyl-6-methoxy-1-(naphthalen-1-ylsulfonyl)-1,2,3,4-tetra-hydroquinoxaline (7-19). White solid (443 mg, 83.1%). ^1H NMR (300 MHz, CDCl_3) δ 8.18 (d, J = 1.8 Hz, 1H), 7.94–7.80 (m, 3H), 7.70–7.55 (m, 3H), 7.45 (dd, J = 8.6, 1.9 Hz, 1H), 7.01 (t, J = 7.4 Hz, 1H), 6.83 (t, J = 7.6 Hz, 2H), 6.55 (d, J = 7.3 Hz, 2H), 6.31 (dd, J = 8.8, 2.7 Hz, 1H), 6.01 (d, J = 2.7 Hz, 1H), 4.09 (s, 2H), 3.91 (t, J = 5.4 Hz, 2H), 3.68 (s, 3H), 2.92 (t, J = 5.4 Hz, 2H).

4.1.29. Synthesis of 4-benzyl-1-(ethylsulfonyl)-6-methoxy-1,2,3,4-tetrahydroquinoxaline (7-20). White solid (342 mg, 80.5%). ^1H NMR (300 MHz, CDCl_3) δ 7.38–7.27 (m, 4H), 7.25–7.20 (m, 2H), 6.27 (d, J = 2.7 Hz, 1H), 6.23 (dd, J = 8.7, 2.7 Hz, 1H), 4.52 (s, 2H), 3.82 (t, J = 5.4 Hz, 2H), 3.69 (s, 3H), 3.47 (t, J = 5.4 Hz, 2H), 2.97 (q, J = 7.4 Hz, 2H), 1.34 (t, J = 7.4 Hz, 3H).

4.1.30. Synthesis of methyl 4-benzyl-1-tosyl-1,2,3,4-tetrahydroquinoxaline-6-carboxylate (7-21). White solid (259 mg, 60.8%). ^1H NMR (300 MHz, CDCl_3) δ 7.78 (d, J = 8.4 Hz, 1H), 7.44 (d, J = 8.2 Hz, 2H), 7.36 (dd, J = 8.4, 1.4 Hz, 1H), 7.31–7.27 (m, 1H), 7.24–7.16 (m, 5H), 6.89–6.79 (m, 2H), 4.37 (s, 2H), 3.88 (t, J = 5.1 Hz, 2H), 3.83 (s, 3H), 2.97 (t, J = 5.2 Hz, 2H), 2.41 (s, 3H).

4.1.31. Synthesis of methyl 4-benzyl-1-((4-methoxyphenyl)sulfonyl)-1,2,3,4-tetrahydroquinoxaline-6-carboxylate (7-22). White solid (280 mg, 53.0%). ^1H NMR (300 MHz, CDCl_3) δ 7.79 (d, J = 8.4 Hz, 1H), 7.48 (d, J = 8.9 Hz, 2H), 7.36 (dd, J = 8.4, 1.6 Hz, 1H), 7.29 (d, J = 1.4 Hz, 1H), 7.24–7.17 (m, 3H), 6.90–6.78 (m, 4H), 4.39 (s, 2H), 3.89 (t, J = 5.0 Hz, 2H), 3.85 (s, 3H), 3.84 (s, 3H), 3.01 (t, J = 5.2 Hz, 2H).

4.1.32. Synthesis of 1-tosyl-1,2,3,4-tetrahydroquinoxaline (I-1). Brown solid (1.60 g, 74.4%). m.p.: 148.3–149.6 °C. HPLC purity: 99.16%. ^1H NMR (300 MHz, CDCl_3) δ 7.63 (dd, J = 8.2, 1.5 Hz, 1H), 7.43 (d, J = 8.3 Hz, 2H), 7.17 (d, J = 8.0 Hz, 2H), 7.00–6.92 (m, 1H), 6.70–6.62 (m, 1H), 6.45 (dd, J = 8.0, 1.4 Hz, 1H), 3.83 (br, 1H), 3.74 (t, J = 5.1 Hz, 2H), 2.88 (t, J = 5.2 Hz, 2H), 2.36 (s, 3H). ^{13}C NMR (75 MHz, CDCl_3) δ 143.73, 137.87, 136.68, 129.70, 127.29, 126.60, 126.22, 121.75, 116.97, 114.77, 43.82, 38.81, 21.59. HRMS (ESI) m/z $[\text{M} + \text{Na}]^+$ calcd for $\text{C}_{15}\text{H}_{16}\text{N}_2\text{NaO}_2\text{S}$ 311.0830, found 311.0823.

4.1.33. Synthesis of 1-((4-methoxyphenyl)sulfonyl)-1,2,3,4-tetrahydroquinoxaline (I-2). Brown solid (1.59 g, 70.4%). m.p.: 112.6–114.2 °C. HPLC purity: 98.09%. ^1H NMR (300 MHz, CDCl_3) δ 7.69 (d, J = 8.0 Hz, 1H), 7.53 (d, J = 8.6 Hz, 2H), 7.01 (t, J = 7.4 Hz, 1H), 6.89 (d, J = 8.6 Hz, 2H), 6.72 (t, J = 7.6 Hz, 1H),



6.50 (d, $J = 7.9$ Hz, 1H), 3.86 (s, 3H), 3.81 (t, $J = 4.9$ Hz, 2H), 2.97 (t, $J = 4.8$ Hz, 2H). ^{13}C NMR (75 MHz, CDCl_3) δ 163.03, 137.87, 131.24, 129.38, 126.63, 126.44, 121.78, 117.04, 114.70, 114.20, 55.60, 43.78, 38.76. HRMS (ESI) m/z $[\text{M} + \text{Na}]^+$ calcd for $\text{C}_{15}\text{H}_{16}\text{N}_2\text{NaO}_3\text{S}$ 327.0779, found 327.0769.

4.1.34. Synthesis of 1-((2-methoxyphenyl)sulfonyl)-1,2,3,4-tetrahydroquinoxaline (I-3). Brown solid (1.64 g, 72.2%). m.p.: 126.1–127.6 °C. HPLC purity: 99.88%. ^1H NMR (300 MHz, CDCl_3) δ 7.98 (dd, $J = 7.9, 1.7$ Hz, 1H), 7.50 (ddd, $J = 8.3, 7.4, 1.7$ Hz, 1H), 7.41 (dd, $J = 8.2, 1.4$ Hz, 1H), 7.08–6.99 (m, 1H), 6.94–6.86 (m, 2H), 6.66–6.59 (m, 1H), 6.53 (dd, $J = 8.0, 1.5$ Hz, 1H), 3.79 (t, $J = 4.9$ Hz, 2H), 3.56 (s, 3H), 3.10 (t, $J = 5.0$ Hz, 2H). ^{13}C NMR (75 MHz, CDCl_3) δ 157.02, 136.84, 134.86, 131.35, 128.18, 125.24, 124.10, 123.91, 120.28, 117.06, 114.52, 112.21, 55.65, 43.93, 40.28. HRMS (ESI) m/z $[\text{M} + \text{H}]^+$ calcd for $\text{C}_{15}\text{H}_{17}\text{N}_2\text{O}_3\text{S}$ 305.0960, found 305.0951.

4.1.35. Synthesis of 1-((3,4-dimethoxyphenyl)sulfonyl)-1,2,3,4-tetrahydroquinoxaline (I-4). Brown solid (1.70 g, 68.4%). m.p.: 135.6–137.1 °C. HPLC purity: 99.18%. ^1H NMR (300 MHz, CDCl_3) δ 7.69 (dd, $J = 8.2, 1.5$ Hz, 1H), 7.29 (dd, $J = 8.6, 2.1$ Hz, 1H), 7.03–6.94 (m, 1H), 6.84 (d, $J = 8.5$ Hz, 1H), 6.75 (d, $J = 2.1$ Hz, 1H), 6.72–6.65 (m, 1H), 6.45 (dd, $J = 8.0, 1.4$ Hz, 1H), 3.90 (s, 3H), 3.77 (t, $J = 5.1$ Hz, 2H), 3.59 (s, 3H), 2.88 (t, $J = 5.2$ Hz, 2H). ^{13}C NMR (75 MHz, CDCl_3) δ 152.61, 148.85, 138.13, 131.23, 126.82, 126.66, 121.75, 120.77, 116.96, 114.59, 110.30, 109.64, 56.12, 55.89, 43.82, 38.38. HRMS (ESI) m/z $[\text{M} + \text{Na}]^+$ calcd for $\text{C}_{16}\text{H}_{18}\text{N}_2\text{NaO}_4\text{S}$ 357.0885, found 357.0876.

4.1.36. Synthesis of 6-methoxy-1-tosyl-1,2,3,4-tetrahydroquinoxaline (I-5). To a solution of 7-1 (350 mg, 0.86 mmol) in methanol (40 mL) was added Raney Ni, the reaction mixture was stirred at 60 °C for 4 h under H_2 , and monitored by TLC (PE : EtOAc = 2 : 1). Then the reaction mixture was filtered with Celite, then the filtrate was concentrated under vacuum to yield the crude product. The crude product was purified by flash column chromatography (PE : EtOAc = 5 : 1) to produce the target compound I-5 (202 mg, 74.3%) as a white solid. m.p.: 117.5–119.1 °C. HPLC purity: 99.97%. ^1H NMR (300 MHz, CDCl_3) δ 7.50 (d, $J = 8.9$ Hz, 1H), 7.40 (d, $J = 8.2$ Hz, 2H), 7.16 (d, $J = 8.1$ Hz, 2H), 6.23 (dd, $J = 8.9, 2.8$ Hz, 1H), 5.97 (d, $J = 2.7$ Hz, 1H), 3.94 (br, 1H), 3.73–3.67 (m, 5H), 2.80 (t, $J = 5.1$ Hz, 2H), 2.35 (s, 3H). ^{13}C NMR (75 MHz, CDCl_3) δ 158.55, 143.72, 139.04, 136.48, 129.72, 127.63, 127.32, 114.86, 103.09, 99.06, 55.25, 43.79, 38.35, 21.61. HRMS (ESI) m/z $[\text{M} + \text{H}]^+$ calcd for $\text{C}_{16}\text{H}_{19}\text{N}_2\text{O}_3\text{S}$ 319.1116, found 319.1110.

The target compounds I-6–I-26 were synthesized following a similar method of compound I-5.

4.1.37. Synthesis of 6-methoxy-1-(*m*-tolylsulfonyl)-1,2,3,4-tetrahydroquinoxaline (I-6). White solid (222 mg, 81.2%). m.p.: 141.8–143.3 °C. HPLC purity: 99.54%. ^1H NMR (300 MHz, CDCl_3) δ 7.50 (d, $J = 8.9$ Hz, 1H), 7.38–7.24 (m, 4H), 6.25 (dd, $J = 8.9, 2.8$ Hz, 1H), 5.98 (d, $J = 2.8$ Hz, 1H), 3.74–3.66 (m, 5H), 2.82 (t, $J = 5.3$ Hz, 2H), 2.30 (s, 3H). ^{13}C NMR (75 MHz, CDCl_3) δ 158.61, 139.28, 139.22, 139.02, 133.63, 128.93, 127.69, 127.57, 124.47, 114.92, 103.10, 99.08, 55.29, 43.82, 38.46, 21.33. HRMS (ESI) m/z $[\text{M} + \text{H}]^+$ calcd for $\text{C}_{16}\text{H}_{19}\text{N}_2\text{O}_3\text{S}$ 319.1116, found 319.1113.

4.1.38. Synthesis of 6-methoxy-1-((4-methoxyphenyl)sulfonyl)-1,2,3,4-tetrahydro-quinoxaline (I-7). White solid

(202 mg, 72.9%). m.p.: 118.1–119.6 °C. HPLC purity: 99.78%. ^1H NMR (300 MHz, CDCl_3) δ 7.53 (d, $J = 8.9$ Hz, 1H), 7.46 (d, $J = 8.9$ Hz, 2H), 6.85 (d, $J = 8.9$ Hz, 2H), 6.27 (dd, $J = 8.9, 2.7$ Hz, 1H), 5.98 (d, $J = 2.7$ Hz, 1H), 3.82 (s, 3H), 3.77–3.70 (m, 5H), 2.86 (t, $J = 5.2$ Hz, 2H). ^{13}C NMR (75 MHz, CDCl_3) δ 162.91, 158.47, 138.87, 131.13, 129.37, 127.82, 115.09, 114.10, 102.99, 99.13, 55.52, 55.22, 43.75, 38.37. HRMS (ESI) m/z $[\text{M} + \text{H}]^+$ calcd for $\text{C}_{16}\text{H}_{19}\text{N}_2\text{O}_4\text{S}$ 335.1066, found 335.1057.

4.1.39. Synthesis of 6-methoxy-1-((3-methoxyphenyl)sulfonyl)-1,2,3,4-tetrahydro-quinoxaline (I-8). White solid (224 mg, 71.3%). m.p.: 147.8–150.3 °C. HPLC purity: 96.01%. ^1H NMR (300 MHz, CDCl_3) δ 7.58 (d, $J = 8.9$ Hz, 1H), 7.31 (t, $J = 7.9$ Hz, 1H), 7.20 (d, $J = 7.8$ Hz, 1H), 7.04 (dd, $J = 7.5, 1.8$ Hz, 1H), 6.98–6.93 (m, 1H), 6.30 (dd, $J = 9.0, 2.7$ Hz, 1H), 5.99 (d, $J = 2.7$ Hz, 1H), 3.79–3.73 (m, 5H), 3.66 (s, 3H), 2.91–2.81 (m, 2H). ^{13}C NMR (75 MHz, CDCl_3) δ 159.70, 158.70, 140.57, 138.90, 129.94, 127.77, 119.75, 119.45, 115.14, 111.43, 103.15, 99.19, 55.48, 55.32, 43.92, 38.42. HRMS (ESI) m/z $[\text{M} + \text{H}]^+$ calcd for $\text{C}_{16}\text{H}_{19}\text{N}_2\text{O}_4\text{S}$ 335.1066, found 335.1058.

4.1.40. Synthesis of 6-methoxy-1-((2-methoxyphenyl)sulfonyl)-1,2,3,4-tetrahydro-quinoxaline (I-9). White solid (252 mg, 80.3%). m.p.: 111.0–112.8 °C. HPLC purity: 99.13%. ^1H NMR (300 MHz, CDCl_3) δ 7.93 (d, $J = 7.8$ Hz, 1H), 7.55–7.45 (m, 1H), 7.32 (d, $J = 8.9$ Hz, 1H), 7.00 (d, $J = 7.5$ Hz, 1H), 6.90 (d, $J = 8.3$ Hz, 1H), 6.21 (dd, $J = 8.9, 2.6$ Hz, 1H), 6.07 (d, $J = 2.6$ Hz, 1H), 3.94 (br, 1H), 3.75–3.66 (m, 5H), 3.56 (s, 3H), 3.01 (t, $J = 5.0$ Hz, 2H). ^{13}C NMR (75 MHz, CDCl_3) δ 157.62, 157.04, 137.99, 134.89, 131.33, 128.03, 125.66, 120.25, 117.28, 112.28, 102.65, 99.36, 55.74, 55.33, 43.73, 39.83. HRMS (ESI) m/z $[\text{M} + \text{H}]^+$ calcd for $\text{C}_{16}\text{H}_{19}\text{N}_2\text{O}_4\text{S}$ 335.1066, found 335.1056.

4.1.41. Synthesis of 1-((3,4-dimethoxyphenyl)sulfonyl)-6-methoxy-1,2,3,4-tetrahydro-quinoxaline (I-10). White solid (256 mg, 80.1%). m.p.: 147.8–149.3 °C. HPLC purity: 99.53%. ^1H NMR (300 MHz, CDCl_3) δ 7.60 (d, $J = 8.9$ Hz, 1H), 7.29 (dd, $J = 8.4, 2.4$ Hz, 1H), 6.88 (d, $J = 8.5$ Hz, 1H), 6.81 (d, $J = 2.0$ Hz, 1H), 6.32 (dd, $J = 8.9, 2.7$ Hz, 1H), 6.00 (d, $J = 2.7$ Hz, 1H), 3.94 (s, 3H), 3.81–3.75 (m, 5H), 3.67 (s, 3H), 2.87 (t, $J = 5.2$ Hz, 2H). ^{13}C NMR (75 MHz, CDCl_3) δ 158.74, 152.55, 148.79, 139.11, 131.19, 128.00, 120.88, 115.16, 110.31, 109.76, 103.10, 99.02, 56.12, 55.93, 55.33, 43.86, 38.17. HRMS (ESI) m/z $[\text{M} + \text{H}]^+$ calcd for $\text{C}_{17}\text{H}_{21}\text{N}_2\text{O}_5\text{S}$ 365.1171, found 365.1165.

4.1.42. Synthesis of 1-((2,4-dimethoxyphenyl)sulfonyl)-6-methoxy-1,2,3,4-tetrahydro-quinoxaline (I-11). White solid (603 mg, 74.3%). m.p.: 116.3–117.5 °C. HPLC purity: 98.28%. ^1H NMR (300 MHz, CDCl_3) δ 7.91 (d, $J = 8.8$ Hz, 1H), 7.40 (d, $J = 8.9$ Hz, 1H), 6.54 (dd, $J = 8.8, 2.3$ Hz, 1H), 6.42 (d, $J = 2.2$ Hz, 1H), 6.28 (dd, $J = 8.9, 2.8$ Hz, 1H), 6.11 (d, $J = 2.8$ Hz, 1H), 3.88 (s, 3H), 3.79–3.72 (m, 5H), 3.58 (s, 3H), 3.10 (t, $J = 5.0$ Hz, 2H). ^{13}C NMR (75 MHz, CDCl_3) δ 164.94, 158.55, 157.51, 137.70, 133.15, 125.89, 120.29, 117.58, 104.19, 102.78, 99.50, 99.29, 55.74, 55.73, 55.34, 43.61, 39.74. HRMS (ESI) m/z $[\text{M} + \text{H}]^+$ calcd for $\text{C}_{17}\text{H}_{21}\text{N}_2\text{O}_5\text{S}$ 365.1171, found 365.1163.

4.1.43. Synthesis of 1-((2,5-dimethoxyphenyl)sulfonyl)-6-methoxy-1,2,3,4-tetrahydro-quinoxaline (I-12). White solid (251 mg, 78.5%). m.p.: 143.6–144.9 °C. HPLC purity: 98.78%. ^1H NMR (300 MHz, CDCl_3) δ 7.48 (d, $J = 3.1$ Hz, 1H), 7.33 (d, $J = 8.9$ Hz, 1H), 7.03 (dd, $J = 9.0, 3.2$ Hz, 1H), 6.84 (d, $J = 9.0$ Hz,



1H), 6.23 (dd, $J = 8.9, 2.7$ Hz, 1H), 6.07 (d, $J = 2.7$ Hz, 1H), 3.95 (br, 1H), 3.78 (s, 3H), 3.76–3.71 (m, 5H), 3.55 (s, 3H), 3.08 (t, $J = 5.1$ Hz, 2H). ^{13}C NMR (75 MHz, CDCl_3) δ 157.65, 152.84, 151.15, 137.89, 128.60, 125.69, 120.63, 117.36, 115.72, 113.66, 102.74, 99.51, 56.25, 56.11, 55.35, 43.81, 39.97. HRMS (ESI) m/z $[\text{M} + \text{H}]^+$ calcd for $\text{C}_{17}\text{H}_{21}\text{N}_2\text{O}_5\text{S}$ 365.1171, found 365.1163.

4.1.44. Synthesis of 4-((6-methoxy-3,4-dihydroquinoxalin-1(2H)-yl)sulfonyl)aniline (I-13). White solid (166 mg, 71.3%). m.p.: 161.5–162.7 °C. HPLC purity: 98.26%. ^1H NMR (300 MHz, CDCl_3) δ 7.50 (d, $J = 8.9$ Hz, 1H), 7.26 (d, $J = 8.8$ Hz, 2H), 6.53 (d, $J = 8.7$ Hz, 2H), 6.24 (dd, $J = 8.9, 2.7$ Hz, 1H), 6.00 (d, $J = 2.7$ Hz, 1H), 4.27 (br, 1H), 3.72 (s, 3H), 3.66 (t, $J = 4.9$ Hz, 2H), 2.83 (t, $J = 5.0$ Hz, 2H). ^{13}C NMR (75 MHz, CDCl_3) δ 158.40, 151.17, 139.20, 129.31, 127.88, 126.86, 115.12, 114.01, 102.96, 99.00, 55.28, 43.66, 38.20. HRMS (ESI) m/z $[\text{M} + \text{H}]^+$ calcd for $\text{C}_{15}\text{H}_{18}\text{N}_3\text{O}_3\text{S}$ 320.1069, found 320.1060.

4.1.45. Synthesis of 6-methoxy-1-((4-(trifluoromethoxy)phenyl)sulfonyl)-1,2,3,4-tetrahydroquinoxaline (I-14). White solid (235 mg, 83.1%). m.p.: 182.0–183.4 °C. HPLC purity: 98.48%. ^1H NMR (300 MHz, CDCl_3) δ 7.58 (d, $J = 8.8$ Hz, 2H), 7.50 (d, $J = 8.9$ Hz, 1H), 7.22 (d, $J = 8.4$ Hz, 2H), 6.26 (dd, $J = 8.9, 2.7$ Hz, 1H), 5.99 (d, $J = 2.7$ Hz, 1H), 3.95 (br, 1H), 3.79–3.64 (m, 5H), 2.88 (t, $J = 5.2$ Hz, 2H). ^{13}C NMR (75 MHz, CDCl_3) δ 158.82, 152.22 (q, $^3J_{\text{C-F}} = 1.8$ Hz), 139.08, 137.81, 129.45, 127.58, 120.70, 120.18 (q, $^1J_{\text{C-F}} = 257.8$ Hz), 114.37, 103.19, 99.12, 55.21, 43.89, 38.62. HRMS (ESI) m/z $[\text{M} + \text{H}]^+$ calcd for $\text{C}_{16}\text{H}_{16}\text{F}_3\text{N}_2\text{O}_4\text{S}$ 389.0783, found 389.0773.

4.1.46. Synthesis of 6-methoxy-1-((4-(trifluoromethyl)phenyl)sulfonyl)-1,2,3,4-tetrahydroquinoxaline (I-15). White solid (214 mg, 66.7%). m.p.: 101.5–103.2 °C. HPLC purity: 99.77%. ^1H NMR (300 MHz, CDCl_3) δ 7.70–7.65 (m, 4H), 7.56 (d, $J = 8.9$ Hz, 1H), 6.31 (dd, $J = 9.0, 2.7$ Hz, 1H), 6.00 (d, $J = 2.7$ Hz, 1H), 3.81 (t, $J = 5.2$ Hz, 2H), 3.75 (s, 3H), 2.89 (t, $J = 5.3$ Hz, 2H). ^{13}C NMR (75 MHz, CDCl_3) δ 158.89, 143.10, 138.76, 134.34 (q, $^2J_{\text{C-F}} = 32.9$ Hz), 127.84, 127.61, 126.12 (q, $^3J_{\text{C-F}} = 3.6$ Hz), 123.23 (q, $^1J_{\text{C-F}} = 271.2$ Hz), 114.45, 103.43, 99.32, 55.30, 44.01, 38.77. HRMS (ESI) m/z $[\text{M} + \text{H}]^+$ calcd for $\text{C}_{16}\text{H}_{16}\text{F}_3\text{N}_2\text{O}_3\text{S}$ 373.0834, found 373.0826.

4.1.47. Synthesis of 1-((4-(tert-butyl)phenyl)sulfonyl)-6-methoxy-1,2,3,4-tetrahydro-quinoxaline (I-16). White solid (224 mg, 69.9%). m.p.: 116.4–118.2 °C. HPLC purity: 96.68%. ^1H NMR (300 MHz, CDCl_3) δ 7.52 (d, $J = 8.9$ Hz, 1H), 7.47 (d, $J = 8.6$ Hz, 2H), 7.39 (d, $J = 8.6$ Hz, 2H), 6.24 (dd, $J = 8.9, 2.7$ Hz, 1H), 6.00 (d, $J = 2.7$ Hz, 1H), 3.95 (br, 1H), 3.75–3.68 (m, 5H), 2.82 (t, $J = 5.1$ Hz, 2H), 1.29 (s, 9H). ^{13}C NMR (75 MHz, CDCl_3) δ 158.46, 156.64, 138.95, 136.53, 127.51, 127.20, 126.04, 115.06, 103.03, 99.19, 55.25, 43.82, 38.51, 35.15, 31.12. HRMS (ESI) m/z $[\text{M} + \text{H}]^+$ calcd for $\text{C}_{19}\text{H}_{25}\text{N}_2\text{O}_3\text{S}$ 361.1586, found 361.1580.

4.1.48. Synthesis of 6-methoxy-1-((3-(trifluoromethyl)phenyl)sulfonyl)-1,2,3,4-tetrahydroquinoxaline (I-17). White solid (258 mg, 79.8%). m.p.: 103.3–104.5 °C. HPLC purity: 99.93%. ^1H NMR (300 MHz, CDCl_3) δ 7.85–7.78 (m, 2H), 7.70 (d, $J = 7.9$ Hz, 1H), 7.58 (d, $J = 7.8$ Hz, 1H), 7.53 (d, $J = 8.9$ Hz, 1H), 6.31 (dd, $J = 8.9, 2.7$ Hz, 1H), 6.00 (d, $J = 2.7$ Hz, 1H), 3.81 (t, $J = 5.2$ Hz, 2H), 3.75 (s, 3H), 2.91 (t, $J = 5.3$ Hz, 2H). ^{13}C NMR (75 MHz, CDCl_3) δ 159.08, 140.58, 139.17, 131.47 (q, $^2J_{\text{C-F}} = 33.2$ Hz), 130.55, 129.87, 129.37 (q, $^3J_{\text{C-F}} = 3.5$ Hz), 127.56, 124.38 (q, $^3J_{\text{C-F}} = 3.7$ Hz), 123.18 (q, $^1J_{\text{C-F}} = 271.3$ Hz), 114.13, 103.40,

99.10, 55.30, 44.00, 38.64. HRMS (ESI) m/z $[\text{M} + \text{H}]^+$ calcd for $\text{C}_{16}\text{H}_{16}\text{F}_3\text{N}_2\text{O}_3\text{S}$ 373.0834, found 373.0828.

4.1.49. Synthesis of 1-((2-fluorophenyl)sulfonyl)-6-methoxy-1,2,3,4-tetrahydroquinoxaline (I-18). White solid (180 mg, 76.6%). m.p.: 141.8–143.1 °C. HPLC purity: 99.37%. ^1H NMR (300 MHz, CDCl_3) δ 7.83–7.71 (m, 1H), 7.59–7.47 (m, 1H), 7.33 (d, $J = 8.9$ Hz, 1H), 7.24–7.16 (m, 1H), 7.16–7.08 (m, 1H), 6.19 (dd, $J = 8.9, 2.7$ Hz, 1H), 6.02 (d, $J = 2.7$ Hz, 1H), 3.92 (br, 1H), 3.80 (t, $J = 5.0$ Hz, 2H), 3.69 (s, 3H), 3.12 (t, $J = 5.1$ Hz, 2H). ^{13}C NMR (75 MHz, CDCl_3) δ 158.80 (d, $^1J_{\text{C-F}} = 255.5$ Hz), 158.25, 138.61, 135.33 (d, $^3J_{\text{C-F}} = 8.3$ Hz), 130.97, 127.77 (d, $^2J_{\text{C-F}} = 14.2$ Hz), 126.17, 124.55 (d, $^3J_{\text{C-F}} = 3.8$ Hz), 117.42 (d, $^2J_{\text{C-F}} = 21.5$ Hz), 115.03, 103.05, 99.36, 55.26, 43.89, 39.74. HRMS (ESI) m/z $[\text{M} + \text{H}]^+$ calcd for $\text{C}_{15}\text{H}_{16}\text{FN}_2\text{O}_3\text{S}$ 323.0866, found 323.0857.

4.1.50. Synthesis of 1-((3,5-difluorophenyl)sulfonyl)-6-methoxy-1,2,3,4-tetrahydro-quinoxaline (I-19). White solid (251 mg, 79.3%). m.p.: 163.2–164.1 °C. HPLC purity: 99.89%. ^1H NMR (300 MHz, CDCl_3) δ 7.54 (d, $J = 8.9$ Hz, 1H), 7.16–7.11 (m, 2H), 7.01 (tt, $J = 8.5, 2.3$ Hz, 1H), 6.33 (dd, $J = 9.0, 2.7$ Hz, 1H), 6.05 (d, $J = 2.7$ Hz, 1H), 3.91 (br, 1H), 3.82 (t, $J = 5.1$ Hz, 2H), 3.79 (s, 3H), 3.01 (t, $J = 5.2$ Hz, 2H). ^{13}C NMR (75 MHz, CDCl_3) δ 162.65 (dd, $^1J_{\text{C-F}} = 253.1$ Hz, $^3J_{\text{C-F}} = 11.5$ Hz), 158.98, 142.70 (t, $^3J_{\text{C-F}} = 8.2$ Hz), 138.85, 127.41, 114.21, 110.99 (d, $^2J_{\text{C-F}} = 18.3$ Hz), 110.86 (d, $^2J_{\text{C-F}} = 18.3$ Hz), 108.39 (t, $^2J_{\text{C-F}} = 24.9$ Hz), 103.48, 99.31, 55.31, 44.07, 38.87. HRMS (ESI) m/z $[\text{M} + \text{H}]^+$ calcd for $\text{C}_{15}\text{H}_{15}\text{F}_2\text{N}_2\text{O}_3\text{S}$ 341.0771, found 341.0763.

4.1.51. Synthesis of 1-((3,4-difluorophenyl)sulfonyl)-6-methoxy-1,2,3,4-tetrahydro-quinoxaline (I-20). White solid (245 mg, 77.3%). m.p.: 109.8–111.4 °C. HPLC purity: 99.90%. ^1H NMR (300 MHz, CDCl_3) δ 7.50 (d, $J = 8.9$ Hz, 1H), 7.43–7.35 (m, 1H), 7.35–7.28 (m, 1H), 7.25–7.15 (m, 1H), 6.28 (dd, $J = 9.0, 2.8$ Hz, 1H), 6.00 (d, $J = 2.8$ Hz, 1H), 3.81–3.73 (m, 5H), 2.94 (t, $J = 5.4$ Hz, 2H). ^{13}C NMR (75 MHz, CDCl_3) δ 158.94, 153.19 (dd, $^1J_{\text{C-F}} = 255.7$ Hz, $^2J_{\text{C-F}} = 12.5$ Hz), 150.03 (dd, $^1J_{\text{C-F}} = 253.0$ Hz, $^2J_{\text{C-F}} = 13.2$ Hz), 138.97, 136.30 (d, $^3J_{\text{C-F}} = 8.6$ Hz), 127.63, 124.49 (dd, $^2J_{\text{C-F}} = 7.4$ Hz, $^3J_{\text{C-F}} = 4.0$ Hz), 118.14 (d, $^2J_{\text{C-F}} = 18.2$ Hz), 117.20 (dd, $^2J_{\text{C-F}} = 19.7$ Hz, $^3J_{\text{C-F}} = 1.5$ Hz), 114.30, 103.38, 99.22, 55.30, 43.98, 38.74. HRMS (ESI) m/z $[\text{M} + \text{H}]^+$ calcd for $\text{C}_{15}\text{H}_{15}\text{F}_2\text{N}_2\text{O}_3\text{S}$ 341.0771, found 341.0764.

4.1.52. Synthesis of 1-((2,6-difluorophenyl)sulfonyl)-6-methoxy-1,2,3,4-tetrahydro-quinoxaline (I-21). White solid (242 mg, 76.6%). m.p.: 146.2–147.5 °C. HPLC purity: 98.32%. ^1H NMR (300 MHz, CDCl_3) δ 7.58–7.47 (m, 1H), 7.43 (d, $J = 9.0$ Hz, 1H), 7.01 (t, $J = 8.5$ Hz, 2H), 6.29 (dd, $J = 9.0, 2.8$ Hz, 1H), 6.09 (d, $J = 2.8$ Hz, 1H), 3.99 (br, 1H), 3.95 (t, $J = 5.0$ Hz, 2H), 3.76 (s, 3H), 3.30 (t, $J = 5.1$ Hz, 2H). ^{13}C NMR (75 MHz, CDCl_3) δ 159.73 (dd, $^1J_{\text{C-F}} = 258.3$ Hz, $^3J_{\text{C-F}} = 3.9$ Hz), 158.22, 138.17, 134.77 (t, $^3J_{\text{C-F}} = 10.9$ Hz), 125.72, 118.04 (t, $^2J_{\text{C-F}} = 16.3$ Hz), 115.05, 113.27 (d, $^2J_{\text{C-F}} = 23.7$ Hz), 113.23 (d, $^2J_{\text{C-F}} = 23.7$ Hz), 103.17, 99.64, 55.28, 44.15, 39.95. HRMS (ESI) m/z $[\text{M} + \text{H}]^+$ calcd for $\text{C}_{15}\text{H}_{15}\text{F}_2\text{N}_2\text{O}_3\text{S}$ 341.0771, found 341.0763.

4.1.53. Synthesis of 6-methoxy-1-(phenylsulfonyl)-1,2,3,4-tetrahydroquinoxaline (I-22). White solid (201 mg, 74.3%). m.p.: 177.6–179.0 °C. HPLC purity: 98.70%. ^1H NMR (300 MHz, CDCl_3) δ 7.56–7.48 (m, 4H), 7.42–7.34 (m, 2H), 6.25 (dd, $J = 8.9, 2.7$ Hz, 1H), 5.97 (d, $J = 2.7$ Hz, 1H), 3.90 (br, 1H), 3.75–3.68 (m, 5H), 2.80 (t, $J = 4.3$ Hz, 2H). ^{13}C NMR (75 MHz, CDCl_3) δ 158.62,



139.39, 139.00, 132.88, 129.08, 127.62, 127.29, 114.77, 103.12, 99.08, 55.27, 43.82, 38.41. HRMS (ESI) m/z $[M + H]^+$ calcd for $C_{15}H_{17}N_2O_3S$ 305.0960, found 305.0953.

4.1.54. Synthesis of 6-methoxy-1-(naphthalen-1-ylsulfonyl)-1,2,3,4-tetrahydroquinoxaline (I-23). White solid (218 mg, 68.5%). m.p.: 177.4–178.8 °C. HPLC purity: 96.41%. 1H NMR (300 MHz, $CDCl_3$) δ 8.24 (s, 1H), 7.93–7.82 (m, 3H), 7.68–7.57 (m, 3H), 7.47 (dd, J = 8.7, 1.7 Hz, 1H), 6.35 (dd, J = 9.0, 2.7 Hz, 1H), 5.98 (d, J = 2.7 Hz, 1H), 3.83 (t, J = 5.1 Hz, 2H), 3.77 (s, 3H), 2.83 (t, J = 4.2 Hz, 2H). ^{13}C NMR (75 MHz, $CDCl_3$) δ 158.68, 138.98, 136.65, 134.81, 132.13, 129.30, 129.25, 128.85, 128.58, 127.94, 127.73, 127.52, 122.75, 115.03, 103.20, 99.16, 55.31, 43.92, 38.57. HRMS (ESI) m/z $[M + H]^+$ calcd for $C_{19}H_{19}N_2O_3S$ 355.1116, found 355.1107.

4.1.55. Synthesis of 1-(ethylsulfonyl)-6-methoxy-1,2,3,4-tetrahydroquinoxaline (I-24). White solid (151 mg, 68.0%). m.p.: 104.8–106.1 °C. HPLC purity: 99.94%. 1H NMR (300 MHz, $CDCl_3$) δ 7.34 (d, J = 8.9 Hz, 1H), 6.23 (dd, J = 8.9, 2.7 Hz, 1H), 6.15 (d, J = 2.7 Hz, 1H), 4.33 (br, 1H), 3.80–3.70 (m, 5H), 3.46 (t, J = 5.3 Hz, 2H), 3.01 (q, J = 7.4 Hz, 2H), 1.36 (t, J = 7.4 Hz, 3H). ^{13}C NMR (75 MHz, $CDCl_3$) δ 158.30, 138.77, 125.83, 115.40, 103.03, 99.52, 55.32, 46.78, 43.53, 40.96, 8.01. HRMS (ESI) m/z $[M + H]^+$ calcd for $C_{11}H_{17}N_2O_3S$ 257.0960, found 257.0955.

4.1.56. Synthesis of methyl 1-tosyl-1,2,3,4-tetrahydroquinoxaline-6-carboxylate (I-25). White solid (69 mg, 35.4%). m.p.: 168.5–170.0 °C. HPLC purity: 99.82%. 1H NMR (300 MHz, $CDCl_3$) δ 7.75 (d, J = 8.6 Hz, 1H), 7.47 (d, J = 8.2 Hz, 2H), 7.35 (dd, J = 8.6, 1.9 Hz, 1H), 7.20 (d, J = 8.0 Hz, 2H), 7.17 (d, J = 2.0 Hz, 1H), 3.94 (s, 1H), 3.88 (s, 3H), 3.82 (t, J = 5.1 Hz, 2H), 3.00–2.91 (m, 2H), 2.38 (s, 3H). ^{13}C NMR (75 MHz, $CDCl_3$) δ 167.01, 144.04, 137.21, 136.37, 129.84, 127.78, 127.23, 125.97, 125.47, 118.29, 115.91, 52.12, 43.79, 38.83, 21.61. HRMS (ESI) m/z $[M + H]^+$ calcd for $C_{17}H_{19}N_2O_4S$ 347.1066, found 347.1057.

4.1.57. Synthesis of methyl 1-((4-methoxyphenyl)sulfonyl)-1,2,3,4-tetrahydroquinoxaline-6-carboxylate (I-26). White solid (68 mg, 30.4%). m.p.: 165.9–167.5 °C. HPLC purity: 99.73%. 1H NMR (300 MHz, $CDCl_3$) δ 7.75 (d, J = 8.6 Hz, 1H), 7.51 (d, J = 8.6 Hz, 2H), 7.34 (dd, J = 8.6, 1.9 Hz, 1H), 7.17 (d, J = 2.0 Hz, 1H), 6.87 (d, J = 8.6 Hz, 2H), 3.88 (s, 3H), 3.85–3.78 (m, 5H), 2.96 (t, J = 5.1 Hz, 2H). ^{13}C NMR (75 MHz, $CDCl_3$) δ 167.02, 163.23, 137.27, 130.92, 129.33, 127.77, 126.01, 125.60, 118.26, 115.89, 114.34, 55.61, 52.12, 43.75, 38.81. HRMS (ESI) m/z $[M + H]^+$ calcd for $C_{17}H_{19}N_2O_5S$ 363.1015, found 363.1006.

4.2. Biological evaluations

4.2.1. *In vitro* cell growth inhibitory assay. The anti-proliferative activities of all target compounds were evaluated by MTT assay. Cells were dispensed in 96-well plates and cultured at 37 °C in a humidified 5% CO_2 overnight. Then the cells were treated with the tested compounds, after 48 h incubation, MTT was added to each well for 1–2 h. The absorbance was evaluated by microplate reader.

4.2.2. *In vitro* tubulin polymerization assay. Fluorescence-based tubulin polymerization kit (BK011P, Cytoskeleton, USA) was used to evaluate the effect of I-7 on tubulin polymerization under the accordance of the protocol of the manufacturer.

Colchicine and paclitaxel were used as reference compounds and DMSO was used as a blank control. All tested compounds were added to black 96-well plate and incubated at 37 °C, then the tubulin reaction mix containing porcine brain tubulin was added to each well and mixed. The fluorescence was monitored in a multimode reader at 37 °C.

4.2.3. Immunofluorescence staining assay. HT-29 cells were treated with tested compounds for 24 h. Then the cells were fixed with 4% formaldehyde, washed with PBS and permeabilized with 0.1% Triton X-100. The blocking agent 5% bovine serum albumin was added to the cells, and the cells were incubated with primary antibody, washed to remove unbound primary antibody and incubated with secondary antibody. The cells were washed with PBS to remove unbound antibody, and stained with Hoechst 33342. Fluorescence microscope was used to detect the immunofluorescence.

4.2.4. Cell cycle analysis. HeLa cells were treated with different concentration of I-7 for 24 h. Then, the cells were washed with PBS, collected, centrifuged, and fixed with ice-cold ethanol. The cells were resuspended in PBS containing RNase, then stained with propidium iodide (PI) in the dark. And the cells were analyzed by flow cytometry using FACS Calibur instrument.

4.2.5. Cell apoptosis assay. HeLa cells were incubated in 6-well plates, then treated with control (DMSO, 0.1%) or I-7 at different concentration for 48 h. The cells were harvested and centrifuged, the pellets resuspended in binding buffer including Annexin-V/FITC and PI, and incubated in the dark, analyzed using flow cytometer.

4.2.6. Molecular docking. Maestro 11.5 was used for predicting the interactions between I-7 and tubulin. The protein was preprocessed using Protein Preparation Wizard and the OPLS3 force field, the grid was generated using as centroid of Workspace ligand with default settings. The 3D structures of I-7 were modeled using the Ligprep module, then docked to the prepared protein by applying the standard precision protocol. The figure was made by PyMOL.

Author contributions

Conceptualization, Tingting Liang and Jianhong Wang; methodology, Jianguo Qi, Yahong Zhang and Jinguang Zhou; software, Yungen Xu; investigation, Haiyang Dong, Lu Lu, Xueting Song and Youkang Li; writing, Tingting Liang; funding acquisition, Tingting Liang, Jianguo Qi and Yahong Zhang. All authors agree to be accountable for all aspects of the work.

Conflicts of interest

The authors report there are no competing interests to declare.

Acknowledgements

This work was supported by the National Natural Science Foundation of China under Grant [81903443], Key Scientific and Technological Project of Henan Province under Grant [212102310316], Doctoral Research Start-up Fee of Henan University under Grant [CJ3050A0240810], Postdoctoral



Research Start-up Fee of Henan University under Grant [FJ3050A0670165], Scientific Research Project of the Institute of Traditional Chinese Medicine of Henan University under Grant [2021YJYZ10].

References

- 1 R. L. Siegel, K. D. Miller, N. S. Wagle and A. Jemal, Cancer statistics, 2023, *Ca-Cancer J. Clin.*, 2023, **73**(1), 17–48.
- 2 M. A. Jordan and L. Wilson, Microtubules as a target for anticancer drugs, *Nat. Rev. Cancer*, 2004, **4**(4), 253–265.
- 3 K. Haider, S. Rahaman, M. S. Yar and A. Kamal, Tubulin inhibitors as novel anticancer agents: an overview on patents (2013-2018), *Expert Opin. Ther. Pat.*, 2019, **29**(8), 623–641.
- 4 D. Adrianzen Herrera, N. Ashai, R. Perez-Soler and H. Cheng, Nanoparticle albumin bound-paclitaxel for treatment of advanced non-small cell lung cancer: an evaluation of the clinical evidence, *Expert Opin. Pharmacother.*, 2019, **20**(1), 95–102.
- 5 P. Yuan, X. Hu, T. Sun, W. Li, Q. Zhang, S. Cui, Y. Cheng, Q. Ouyang, X. Wang, Z. Chen, M. Hiraiwa, K. Saito, S. Funasaka and B. Xu, Eribulin mesilate versus vinorelbine in women with locally recurrent or metastatic breast cancer: A randomised clinical trial, *Eur. J. Cancer*, 2019, **112**, 57–65.
- 6 W. Li, H. Zhang, Y. G. Assaraf, K. Zhao, X. Xu, J. Xie, D. H. Yang and Z. S. Chen, Overcoming ABC transporter-mediated multidrug resistance: Molecular mechanisms and novel therapeutic drug strategies, *Drug Resistance Updates*, 2016, **27**, 14–29.
- 7 M. Liu, M. Fu, X. Yang, G. Jia, X. Shi, J. Ji, X. Liu and G. Zhai, Paclitaxel and quercetin co-loaded functional mesoporous silica nanoparticles overcoming multidrug resistance in breast cancer, *Colloids Surf., B*, 2020, **196**, 111284.
- 8 R. Gaspari, A. E. Prota, K. Bargsten, A. Cavalli and M. O. Steinmetz, Structural basis of cis- and trans-combretastatin binding to tubulin, *Chem*, 2017, **2**(1), 102–113.
- 9 J. Wang, D. D. Miller and W. Li, Molecular interactions at the colchicine binding site in tubulin: An X-ray crystallography perspective, *Drug Discovery Today*, 2022, **27**(3), 759–776.
- 10 G. J. Brouhard and L. M. Rice, The contribution of alpha beta-tubulin curvature to microtubule dynamics, *J. Cell Biol.*, 2014, **207**(3), 323–334.
- 11 M. Gao, Y. Yang, Y. Gao, T. Liu, Q. Guan, T. Zhou, Y. Shi, M. Hao, Z. Li, D. Zuo, W. Zhang and Y. Wu, The anti-MDR efficacy of YAN against A549/Taxol cells is associated with its inhibition on glycolysis and is further enhanced by 2-deoxy-d-glucose, *Chem.-Biol. Interact.*, 2022, **354**, 109843.
- 12 M. S. Lin, T. M. Hong, T. H. Chou, S. C. Yang, W. C. Chung, C. W. Weng, M. L. Tsai, T. J. R. Cheng, J. J. W. Chen, T. C. Lee, C. H. Wong, R. J. Chein and P. C. Yang, 4(1H)-quinolonederivatives overcome acquired resistance to anti-microtubule agents by targeting the colchicine site of beta-tubulin, *Eur. J. Med. Chem.*, 2019, **181**, 111584.
- 13 W. Yan, T. Yang, J. H. Yang, T. J. Wang, Y. M. Yu, Y. X. Wang, Q. Chen, P. Bai, D. Li, H. Y. Ye, Q. Qiu, Y. Z. Zhou, Y. G. Hu, S. Y. Yang, Y. Q. Wei, W. M. Li and L. J. Chen, SKLB060 reversibly binds to colchicine site of tubulin and possesses efficacy in multidrug-resistant cell lines, *Cell. Physiol. Biochem.*, 2018, **47**(2), 489–504.
- 14 C. Dumontet and M. A. Jordan, Microtubule-binding agents: a dynamic field of cancer therapeutics, *Nat. Rev. Drug Discovery*, 2010, **9**(10), 790–803.
- 15 R. Kaul, A. L. Risinger and S. L. Mooberry, Microtubule-targeting drugs: More than antimetotics, *J. Nat. Prod.*, 2019, **82**(3), 680–685.
- 16 F. F. Qi, J. Zhou and M. Liu, Microtubule-interfering agents, spindle defects, and interkinetochore tension, *J. Cell. Physiol.*, 2020, **235**(1), 26–30.
- 17 E. C. McLoughlin and N. M. O'Boyle, Colchicine-binding site inhibitors from chemistry to clinic: A review, *Pharmaceuticals*, 2020, **13**(1), 8.
- 18 C. Wang, Y. Li, T. Liu, Z. Wang, Y. Zhang, K. Bao, Y. Wu, Q. Guan, D. Zuo and W. Zhang, Design, synthesis and evaluation of antiproliferative and antitubulin activities of 5-methyl-4-aryl-3-(4-arylpiperazine-1-carbonyl)-4H-1,2,4-triazoles, *Bioorg. Chem.*, 2020, **104**, 103909.
- 19 L. Li, S. B. Jiang, X. X. Li, Y. Liu, J. Su and J. J. Chen, Recent advances in trimethoxyphenyl (TMP) based tubulin inhibitors targeting the colchicine binding site, *Eur. J. Med. Chem.*, 2018, **151**, 482–494.
- 20 L. Y. Xia, Y. L. Zhang, R. Yang, Z. C. Wang, Y. D. Lu, B. Z. Wang and H. L. Zhu, Tubulin inhibitors binding to colchicine-site: A review from 2015 to 2019, *Curr. Med. Chem.*, 2020, **27**(40), 6787–6814.
- 21 T. Y. Ji, X. E. Jian, L. Chen, W. B. Zeng, X. S. Huo, M. X. Li, P. Chen, Y. Q. Zhang, W. W. You and P. L. Zhao, Discovery of novel 6-p-tolyl-3-(3,4,5-trimethoxybenzyl)-7H-1,2,4-triazolo 3,4-b 1,3,4 thiadiazine derivative as a potent tubulin inhibitor with promising in vivo antitumor activity, *Eur. J. Med. Chem.*, 2023, **256**, 11.
- 22 W. F. Ma, P. Chen, X. S. Huo, Y. F. Ma, Y. H. Li, P. C. Diao, F. Yang, S. Q. Zheng, M. J. Hu, W. W. You and P. L. Zhao, Development of triazolothiadiazine derivatives as highly potent tubulin polymerization inhibitors: Structure-activity relationship, in vitro and in vivo study, *Eur. J. Med. Chem.*, 2020, **208**, 15.
- 23 S. Apaydin and M. Torok, Sulfonamide derivatives as multi-target agents for complex diseases, *Bioorg. Med. Chem. Lett.*, 2019, **29**(16), 2042–2050.
- 24 Y. C. Wan, G. Q. Fang, H. J. Chen, X. Deng and Z. L. Tang, Sulfonamide derivatives as potential anti-cancer agents and their SARs elucidation, *Eur. J. Med. Chem.*, 2021, **226**, 113837.
- 25 R. Ghomashi, S. Ghomashi, H. Aghaei and A. R. Massah, Recent advances in biological active sulfonamide based hybrid compounds Part A: Two-component sulfonamide hybrids, *Curr. Med. Chem.*, 2023, **30**(4), 407–480.
- 26 S. C. He, H. Z. Zhang, H. J. Zhang, Q. Sun and C. H. Zhou, Design and synthesis of novel sulfonamide-derived



- triazoles and bioactivity exploration, *Med. Chem.*, 2020, **16**(1), 104–118.
- 27 J. R. A. Diaz, G. E. Cami, M. Liu-Gonzalez, D. R. Vega, D. Vullo, A. Juarez, J. C. Pedregosa and C. T. Supuran, Salts of 5-amino-2-sulfonamide-1,3,4-thiadiazole, a structural and analog of acetazolamide, show interesting carbonic anhydrase inhibitory properties, diuretic, and anticonvulsant action, *J. Enzyme Inhib. Med. Chem.*, 2016, **31**(6), 1102–1110.
 - 28 P. V. L. Mang, J. C. Hui, R. S. J. Tan, M. S. Hasan, Y. M. Choo, M. F. Abosamak and K. T. Ng, The diuretic effect of adding aminophylline or theophylline to furosemide in pediatric populations: a systematic review, *Eur. J. Pediatr.*, 2023, **182**(1), 1–8.
 - 29 W. He, G. Yuan, Y. Han, Y. C. Yan, G. Li, C. C. Zhao, J. S. Shen, X. R. Jiang, C. Chen, L. Ni and D. W. Wang, Glimepiride use is associated with reduced cardiovascular mortality in patients with type 2 diabetes and chronic heart failure: a prospective cohort study, *Eur. J. Prev. Cardiol.*, 2023, **30**(6), 474–487.
 - 30 M. Talpaz and J. J. Kiladjian, Fedratinib, a newly approved treatment for patients with myeloproliferative neoplasm-associated myelofibrosis, *Leukemia*, 2021, **35**(1), 1–17.
 - 31 J. V. Kaczmarek, C. M. Bogan, J. M. Pierce, Y. K. Tao, S. C. Chen, Q. Liu, X. Liu, K. L. Boyd, M. W. Calcutt, T. M. Bridges, C. W. Lindsley, D. L. Friedman, A. Richmond and A. B. Daniels, Intravitreal HDAC inhibitor belinostat effectively eradicates vitreous seeds without retinal toxicity in vivo in a rabbit retinoblastoma model, *Invest. Ophthalmol. Visual Sci.*, 2021, **62**(14), 8.
 - 32 A. C. Ketron, W. A. Denny, D. E. Graves and N. Osheroff, Amsacrine as a topoisomerase II poison: importance of drug-DNA interactions, *Biochemistry*, 2012, **51**(8), 1730–1739.
 - 33 J. Qi, H. Dong, J. Huang, S. Zhang, L. Niu, Y. Zhang and J. Wang, Synthesis and biological evaluation of N-substituted 3-oxo-1,2,3,4-tetrahydro-quinoxaline-6-carboxylic acid derivatives as tubulin polymerization inhibitors, *Eur. J. Med. Chem.*, 2018, **143**, 8–20.
 - 34 J. Qi, J. Huang, X. Zhou, W. Luo, J. Xie, L. Niu, Z. Yan, Y. Luo, Y. Men, Y. Chen, Y. Zhang and J. Wang, Synthesis and biological evaluation of quinoxaline derivatives as tubulin polymerization inhibitors that elevate intracellular ROS and triggers apoptosis via mitochondrial pathway, *Chem. Biol. Drug Des.*, 2019, **93**(4), 617–627.
 - 35 T. Liang, X. Zhou, L. Lu, H. Dong, Y. Zhang, Y. Xu, J. Qi, Y. Zhang and J. Wang, Structure activity relationships and antiproliferative effects of 1,2,3,4-H-quinoxaline derivatives as tubulin polymerization inhibitors, *Bioorg. Chem.*, 2021, **110**, 104793.
 - 36 A. Daina, O. Michielin and V. Zoete, SwissADME: a free web tool to evaluate pharmacokinetics, drug-likeness and medicinal chemistry friendliness of small molecules, *Sci. Rep.*, 2017, **7**, 42717.

